University of Nevada, Reno

Production of Renewable Diesel Fuel via Hofer-Moest Electrochemical Decarboxylation of Free Fatty Acids

A thesis submitted in partial fulfillment of the
requirements for the degree of Master of Science in
Chemical Engineering

By
Cody James Wagner

Dr. Charles J. Coronella/Thesis Advisor

May, 2012

We recommend that the thesis
prepared under our supervision by

CODY JAMES WAGNER

entitled

**Production Of Renewable Diesel Fuel Via Hofer-Moest
Electrochemical Decarboxylation Of Free Fatty Acids**

be accepted in partial fulfillment of the
requirements for the degree of

MASTER OF SCIENCE

Charles J. Coronella, Ph.D., Advisor

Hongfei Lin, Ph.D., Committee Member

Thomas W. Bell, Ph.D., Graduate School Representative

Marsha H. Read, Ph. D., Dean, Graduate School

May, 2012

Production of Renewable Diesel Fuel via Hofer-Moest Electrochemical Decarboxylation of Free Fatty Acids

Abstract

The industrialization and modernization of some of the world's poorest, densely populated countries, coupled with the limited supply of petroleum globally, has created an escalating energy problem. Advanced biofuels, derived from biologically grown feedstocks, are renewable fuels which provide a drop-in replacement for petroleum. One potential conversion pathway to turn lipid-based biomass feedstocks into a renewable diesel fuel is through non-Kolbe electrolysis. When performed on a graphite surface, electrolysis of free fatty acid (FFA) salts in an alcoholic electrolyte at potentials of at least 2.5 V/cell causes a two-electron Hofer-Moest decarboxylation. This reaction produces several hydrocarbons, ethers, and esters at a current efficiency of approximately 73.9%. Using 2011 electricity statistics, an average electrical energy cost to produce one gallon of the fuel from pure oleic acid is $0.383. From analysis of a full factorial design of experiment, higher ion concentrations and lower temperatures optimize the production rate and current efficiency of the reaction, while a maximal percentage of hydrocarbons are produced in neutral solutions. In comparison to biodiesel, this fuel product has better heating values and cold flow properties but demonstrates worse oxidative stability. An advantage of this electrochemical process is the robustness of feedstocks that can be used, which includes algae oils, high FFA wastes such as brown and yellow grease, and biodiesel waste FFA salts.

Acknowledgements

First and foremost, my advisor, Dr. Charles Coronella, made this thesis possible. His leadership and guidance has made my graduate student experience valuable and enjoyable. I will be forever indebted for his generous contributions in my personal and professional life.

Special thanks to Dr. Rainer Busch, whose creativity in electrochemical research generated the concept for this project. His contributions and input have been invaluable. His donations of funds, equipment, and chemicals are appreciated.

Dr. Glenn Miller has generously donated lab space and equipment for the duration of the project. His input and assistance, especially in the analytical chemistry aspects of this project, were crucial to this thesis. Thanks to his assistants, Patrick Freeze and Jeffrey Cullen, for their help as well.

Students Micheil Jones and Diane Mar have dedicated countless hours of research to this project. Their responsible attitudes and creative contributions have been vital. Special thanks and congratulations to Micheil for continuing his hard work, even while welcoming his first child, Branch, into the world this past April.

Fellow graduate students Mohammed (Toufiq) Reza, Kevin Schmidt, York Smith, Jason Hastings, Joan Lynam, Jason Strull, Orion Hanbury, and Tapas Acharjee, among others, have all contributed to my success, both in academic classes and research. It has been a pleasure to share my graduate experience with this group.

Special thanks to Dr. Hongfei Lin and Dr. Thomas Bell for serving on my thesis committee. I would also like to appreciate the gracious contributions from Dr. Dave Quilici, Dr. Victor Vasquez, Dr. Dev Chidambaram, Dr. Alan Fuchs, and other members

of the Chemical and Materials Engineering Department for their assistance throughout my undergraduate and graduate career at the University of Nevada, Reno.

Dr. Robert (Bob) Dunn with USDA's National Center for Agricultural Utilization Research (NCAUR) has been incredibly helpful, donating his time and resources to test fuels for this project. His contributions are greatly appreciated.

Finally, I would like to thank all of my friends, family, and co-workers for their support. I could not imagine having a better support system around me. I would like to dedicate this work to the memory of my mother, who lost her battle to cancer six years ago.

CONTENT

FIGURES

TABLES

Chapter 1 – Introduction

As the world's population increases and less developed countries advance technologically, an ever-increasing amount of energy is needed. Much of the current energy comes from non-renewable fossil fuels, of which the world has a diminishing supply. The consumption of these fuels increases carbon emissions into the atmosphere, which causes much uncertainty about climate change. In order to advance towards a sustainable global economy and ease climate change fears, more renewable energy sources need to be developed.

This reality is especially true for liquid transportation fuels. Concerns about petroleum oil supply are rampant, especially for non-OPEC (Organization of the Petroleum Exporting Countries) countries. These countries have had to develop other petroleum-related technologies, such as oil sands extraction, to try to keep up with demand. Safety and environmental concerns are currently being raised for these new methods [1]. Nevertheless, the price of oil per gallon has nearly tripled since 2004, and non-OPEC production has remained approximately flat during that same time period, showing that maximum production, or "peak oil", might already be a reality [2].

The development of methods for producing biofuels could provide at least part of a solution to the continual consumption of petroleum fuels, both from an economical and environmental standpoint. Here in the US, if biomass feedstocks for biofuel conversion technologies can be produced cheaply and with a positive net energy gain (NEG), a more reliable fuel production supply could develop, helping to stabilize some of the fluctuating prices seen at the pump. Overseas conflicts and other political situations in OPEC

countries, in addition to market-based speculation, usually out of the reaches of control for the US, are often to blame for the fluctuations [3]. Biofuels would theoretically only release carbon which was originally taken out of the atmosphere by photosynthesis, making the biofuels "carbon neutral" and helping to calm fears of climate change [4]. In this project, the effectiveness of an electrochemical biofuel conversion technology is studied, which has the potential to turn cheap, renewable feedstocks and wastes into a steady supply of green diesel fuel for the future.

1.1 Petroleum Fuels

Crude petroleum is normally sent to a refinery, where it is separated into three different fractions: light distillates, middle distillates, and heavy distillates. These distillates are then further processed through methods such as "cracking", where heavier molecules are split into lighter ones, and "alkylation", which does the opposite. Gasoline is produced from the light distillate fraction, while diesel fuel comes from the middle distillates, making it a heavier fuel with a higher boiling point than regular gasoline [5].

1.1.1 Composition and Properties

Petroleum products, such as gasoline and diesel fuel, are composed primarily of hydrocarbons. These molecules release a maximal amount of energy upon combustion, on both a mass and volumetric basis. A typical table of bond energies, as shown in Table 1.1, can be used to explain this energy [6]. During combustion, bonds are initially broken, an endothermic process. The carbon-carbon, carbon-hydrogen, and oxygen-

oxygen bonds do not require a large endotherm to break, in comparison to many other covalent bonds. During combustion, water and carbon dioxide form as products. The formation of bonds in these molecules is exothermic, releasing energy. From the table of bond energies, oxygen-hydrogen single bonds and carbon-oxygen double bonds are highly energetic, causing the large exotherm observed during combustion. The total heat of combustion is the difference between the exothermic bond formation and the endothermic bond destruction. On a molar basis, this heat of combustion for hydrocarbons is much greater than for molecules containing oxygen atoms [7]. When considering fuels on a mass or volume basis, hydrocarbons are even more energy dense because oxygen has a greater atomic mass and volume. This high energy density contributes to better fuel efficiency, commonly measured in miles per gallon in the United States, for hydrocarbon fuels compared to that for oxygenated fuels [8]. The biggest difference between petroleum fuels and biofuels, discussed in section 1.2, is oxygen content, as biofuels are usually between 10% and 45% oxygen (by mass), causing inferior heats of combustion and fuel efficiency [9].

Bonded atoms	Energy (kJ/mol)	Bonded atoms	Energy (kJ/mol)
C-C	347	C=O	745
C-H	413	O-H	467
C=C	614	H-H	432
C-O	358	N-N	160
C-N	305	O-O	146

Table 1.1: Dissociation energies of several common molecular bonds [6]

Gasoline is the fuel of choice for most cars today. It is comprised of primarily hydrocarbons between four and ten carbons in size. This includes paraffins, olefins, and cyclic/aromatic molecules, all of which are compatible with the gasoline internal combustion engine [10]. A key engine performance indicator for gasoline is the octane number, a quantitative measure of the "antiknock" properties. Knock is caused when molecules prematurely combust during pressurization in these engines and is undesirable for gasoline fuel. A higher octane number signifies a combination of molecules which can be further compressed without combusting, making an engine's pressurized combustion process more efficient. N-heptane is given an octane number of 0, while iso-octane (2,2,4-trimethylpentane) has the reference octane number of 100. In a fuel composed of only these two molecules, the octane number would be equivalent to the volume percentage of iso-octane [11, 12]. With the normal blend of many different components in gasoline, each molecule is assigned an octane number based on the average of a research octane number (RON) and motor octane number (MON), which are based on two different ASTM standard tests [13, 14]. The overall octane number of a fuel can be calculated by summing the product of each component's volume fraction and octane number.

n-heptane   2,2,4-trimethylpentane

Octane Number: 0   **Octane Number: 100**
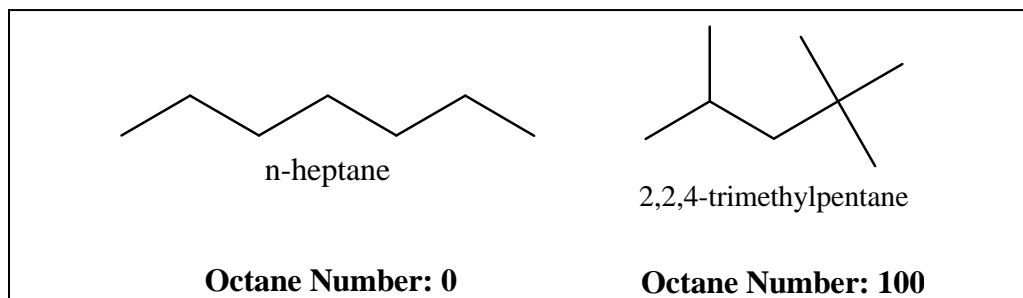
Figure 1.1: Octane numbers for n-heptane and iso-octane (2,2,4-trimethylpentane)

This antiknocking property, which is so important in gasoline, is not as critical in diesel fuel. This is because diesel engines do not pressurize the fuel. Instead, they heat the incoming air by contracting and pressurizing it, and then inject the diesel fuel. One of the important ratings for diesel fuel is the cetane number (CN). This is a measure of the ignition delay of a fuel, which is the amount of time from injection to ignition [15, 16]. Low CN diesel fuels can experience knocking as a result of long ignition delays. An ASTM standard test is used to measure the CN with a standardized engine. Hexadecane ($C_{16}H_{34}$), also known as "cetane", has been assigned the reference cetane number of 100 as an ideal diesel fuel. On the other hand, 2,2,4,4,6,8,8-heptamethylnonane, nicknamed "isocetane", has been assigned a reference CN of 15. N-paraffins decrease in cetane number as the length of their carbon chain decreases. For example, n-octane has a cetane number of 64. Branched, cyclic, and aromatic structures also have lower cetane numbers, while straight-chain hydrocarbons with more than 16 carbons have cetane numbers greater than 100 [17]. Typical values for cetane number of petroleum diesel are between 40 and 65 [16, 18], with increasing number signifying better fuel quality. Other important properties of diesel fuel include viscosity, density, lubricity, and cold flow. Diesel fuel has a complex molecular composition, containing roughly 65-85% aliphatic hydrocarbons, 5-30% aromatic hydrocarbons, and a small fraction of olefins [19]. These hydrocarbons usually contain 10 to 25 carbons, corresponding to the range expected in the middle distillate fraction in crude oil [20].

1.1.2   Projections and Economics

According to the Energy Information Administration (EIA), production from domestic refineries and blenders averaged 18.6 million barrels per day for all petroleum-based fuels in 2011. From this, 9.0 million barrels per day (48.5%) were refined for gasoline and 4.5 million barrels per day (24.1%) were for distillate fuel oil, which included diesel and blended renewable diesel fuels [21]. The graph below shows EIA data for average net production from refineries and blenders since 2000. A fairly consistent increase can be noted in that time range.
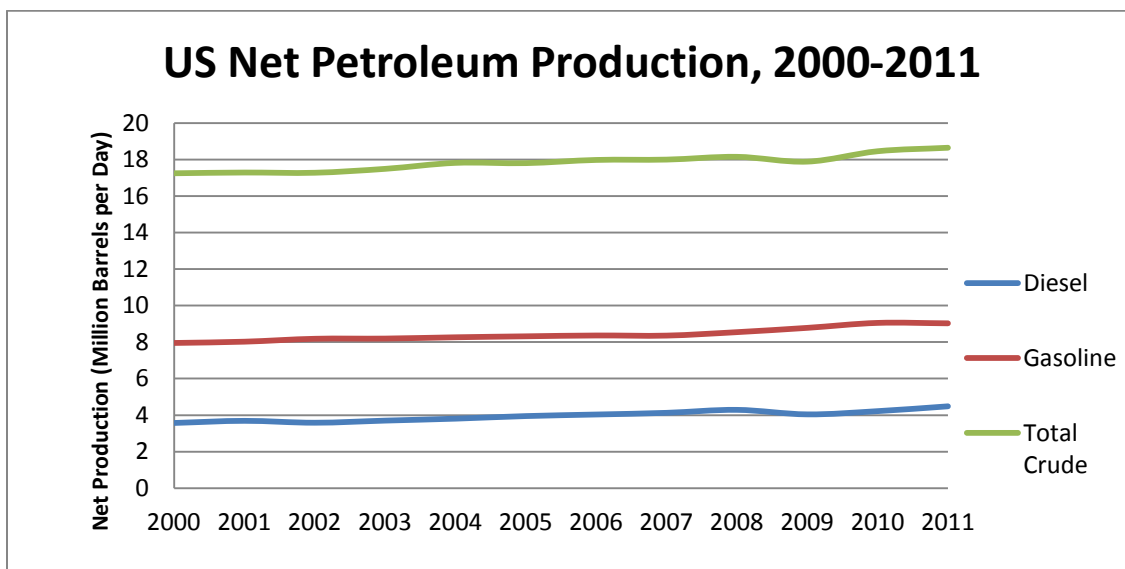
Figure 1.2: EIA Data for Domestic Petroleum Production, 2000-2011 [20]

The EIA also makes future predictions about fuel consumption in its publication of "Annual Energy Outlook" (AEO). While domestic oil consumption is not predicted to change drastically, the global outlook does exhibit an upward trend, as shown in Figure 1.3. This increased consumption is expected as some of the poor, population-dense countries modernize and industrialize.
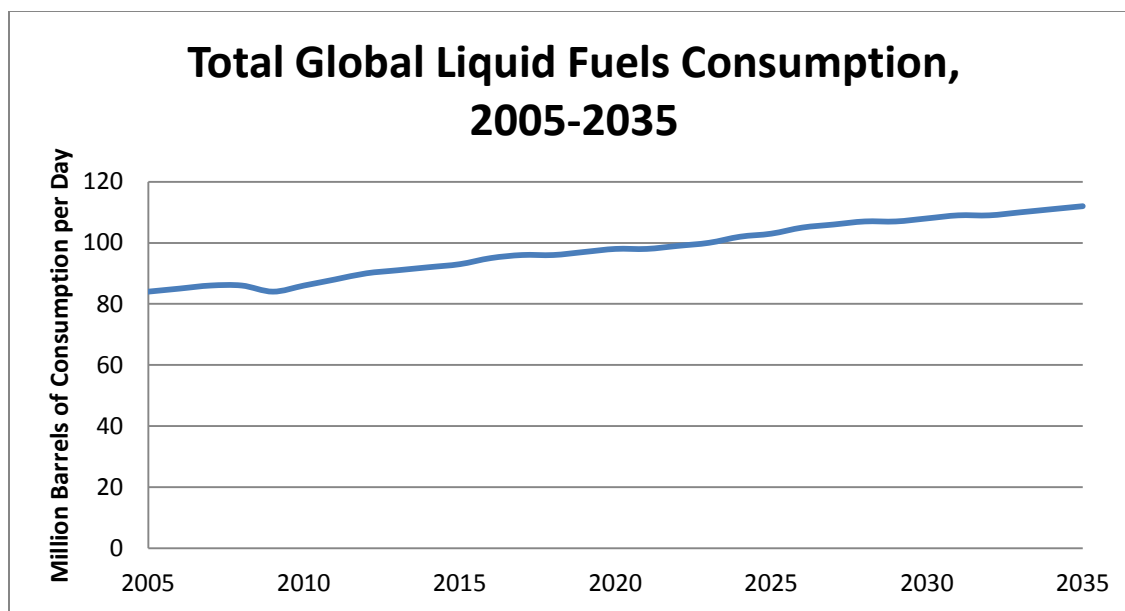
Figure 1.3: EIA data and predictions for global fuels consumption [22]

From an economic perspective, another important factor relating to fuel is price volatility. Higher prices may curb the trend of increasing fuel consumption, while lower prices will encourage greater consumption. Examination of average yearly gasoline and diesel prices in the US in Figure 1.4 reveals much instability. This instability makes pricing predictions very difficult to make. If "peak oil" has been reached or will occur in the near future, a limited crude oil supply will undoubtedly cause large price increases. However, as seen between 2008 and 2009, a price decrease is also possible, depending upon a plethora of global factors. The EIA has published three predictions in its most recent Annual Energy Outlook, *AEO2012*. One is based on an *AEO2012 Reference Case*, while the other two are based on higher and lower oil prices than the reference case, as seen in Figure 1.5 [24].

US Average Fuel Price, 2000-2011
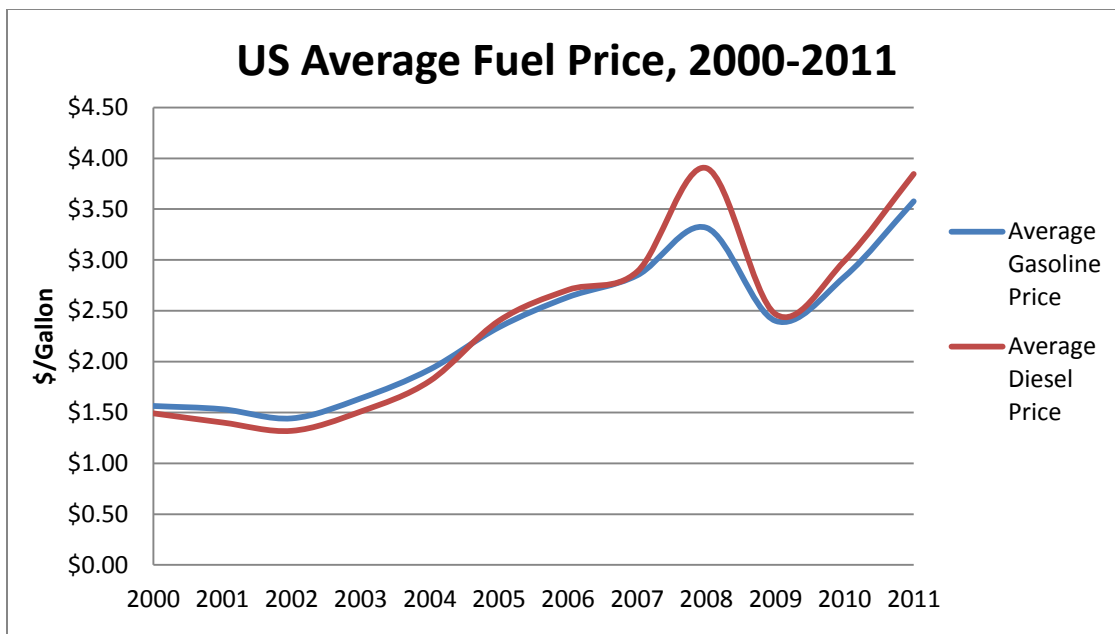
Figure 1.4: Average yearly domestic fuel prices, 2000-2011 [23]
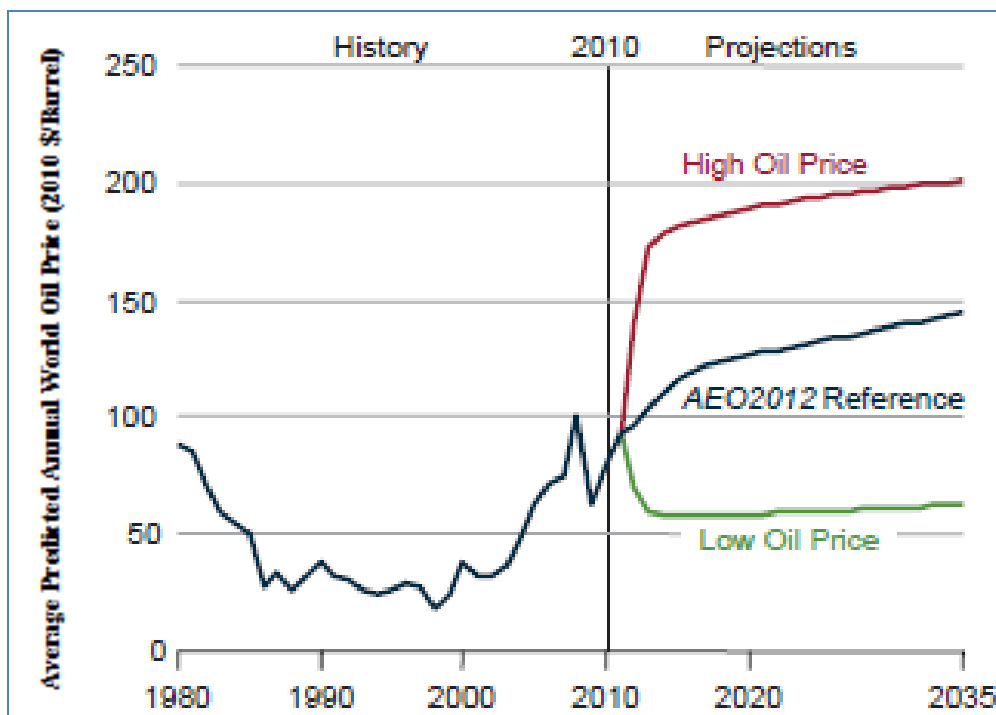
Figure 1.5: Three predictions for future oil prices based on EIA's three different

reference scenarios in its Annual Energy Outlook 2012 [24]

1.1.3 Carbon Emissions

The continual consumption of fossil fuels has caused a massive rise in greenhouse gas (GHG) emissions in recent years, which has prompted many climate change and health fears [25]. In Figure 1.6 below, carbon dioxide emissions are shown since 1990 from both Organization for Economic Cooperation and Development[1] (OECD) countries and non-OECD countries. Emission predictions are also made through 2035. While the OECD countries' emissions do not increase substantially, the modernization and industrialization of developing countries causes their emission levels to nearly double from 2005 numbers, leading to very serious concerns.
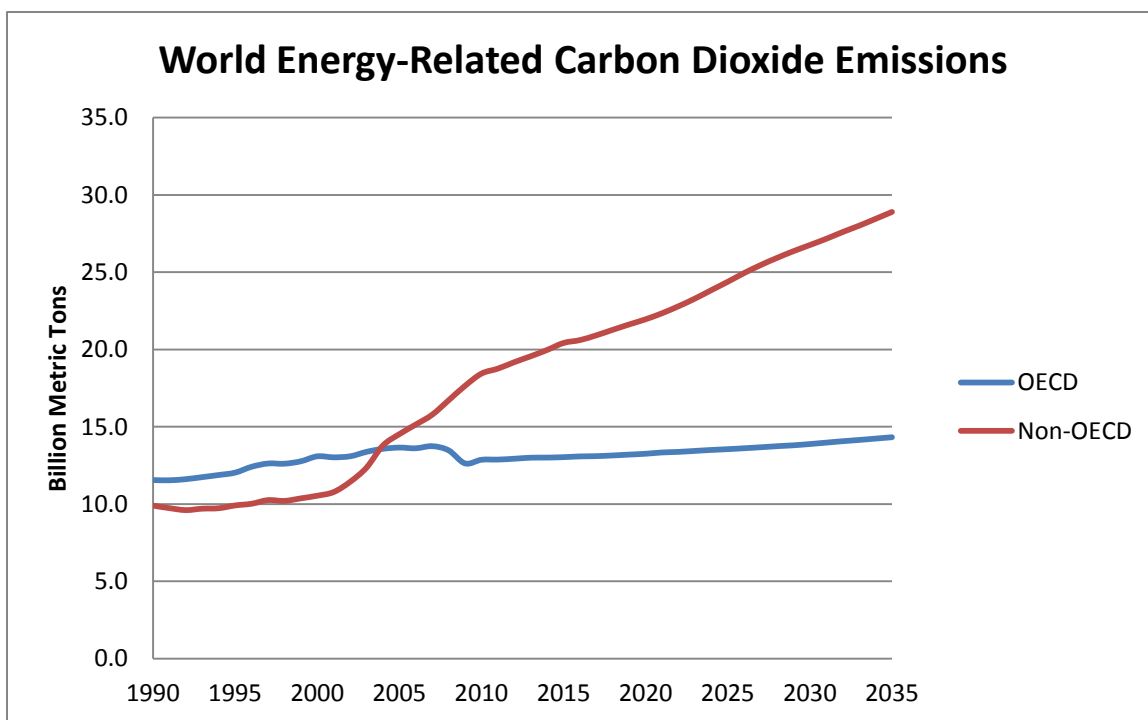
Figure 1.6: Global carbon dioxide emissions, 1990-2035 (predicted) [26]

_____

[1] The OECD is composed of 34 member countries, consisting mainly of European and North American technologically advanced nations.

1.2 Biofuels

With the consumption of petroleum fuels sparking ongoing concerns about dwindling supply and climate change, much research is now being devoted to "biofuels". These are fuels produced from biomass feedstocks. They will still release carbon dioxide when combusted, but their carbon cycle is more favorable, as the carbon dioxide released into the atmosphere was pulled from the atmosphere during photosynthesis [4]. In nearly all cases, there will still be a net carbon release, as inputs such as deforestation, agricultural inputs, and fuel processing must be taken into account [27].

The most recent statistics provided by the EIA through 2009 show a large increase in production of alternative and replacement fuels, which are primarily biofuels [28]. This increase is based both on total production and ratio of renewable fuels to non-renewable fuels, as shown in Figures 1.7 and 1.8. With a greater emphasis on developing sustainable fuels and more government incentives, there is hope that this trend will continue, both domestically and globally. The Energy Independence and Security Act of 2007 established annual Renewable Fuel Standards (RFS) to be set based on EIA predictions. The targets of 15.2 billion gallons of renewable fuels and a ratio of 9.23% (renewable fuel volume to non-renewable fuel volume) were recently set for 2012 [29]. These goals are approximately double 2008 levels.
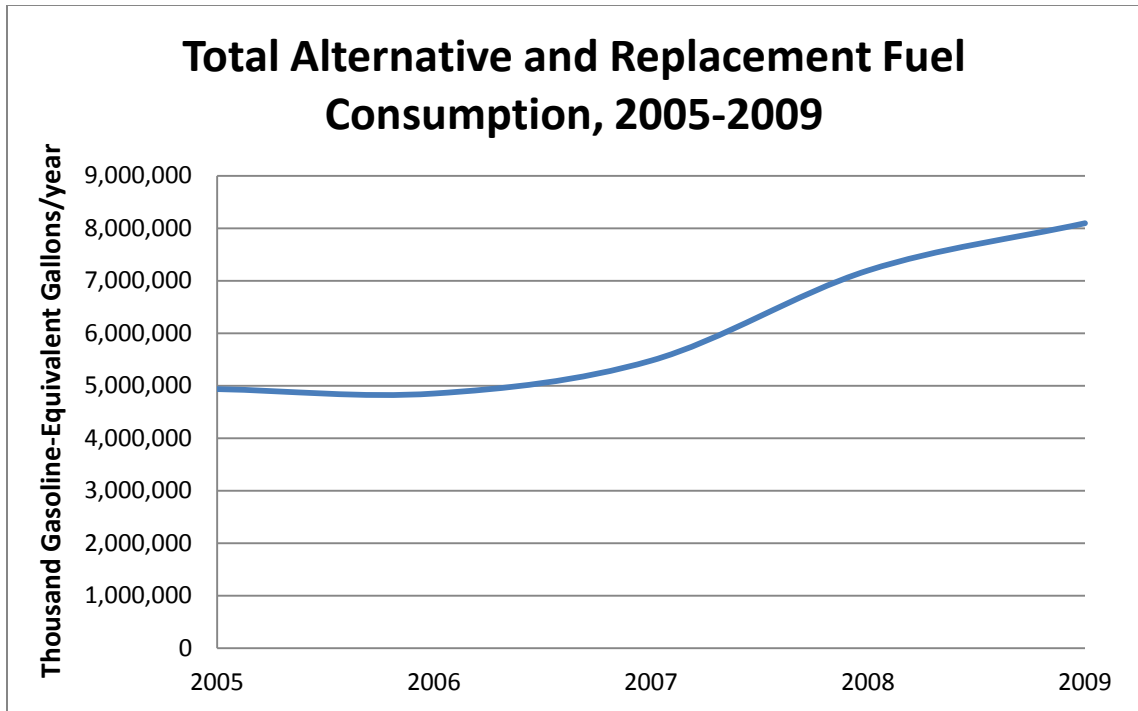
Figure 1.7: Increase of renewable fuel production, 2005-2009 [28]
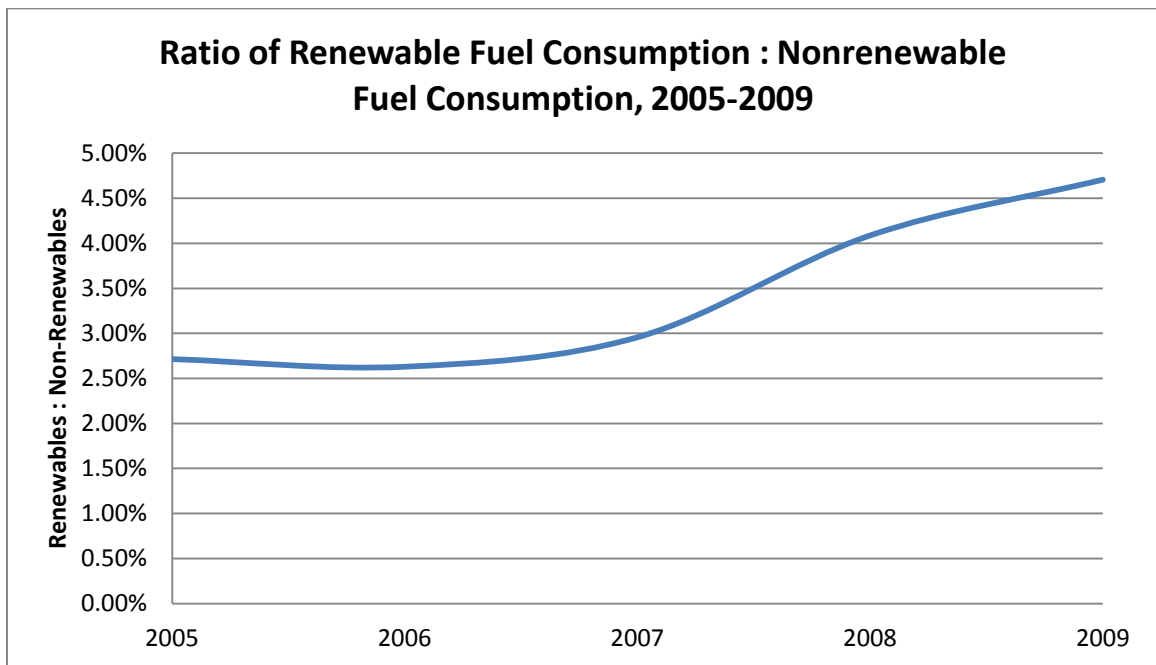
Figure 1.8: Increase in ratio of renewable fuels to non-renewables, following

approximately the same trend as production [28]

1.2.1   First Generation Biofuels

Almost all biofuels commercially available today are considered "first generation". Bio-ethanol accounts for the bulk of first-generation production, while smaller percentages of biodiesel and biogas are included in this category as well [30]. Although these fuels are currently considered the most economical of the renewable fuel options, there are many concerns with production. A key problem is that the net energy balance around these production processes is oftentimes not favorable when accounting for all the process inputs. Also, the "food vs. fuel" debate gains traction when food is sacrificed for energy production, causing supply shortages and raising prices [31]. Domestic corn ethanol production has run into both these problems. The general perception of the unsustainability and negative net energy balance around corn ethanol production has hurt the reputation of renewable fuels in recent years [32]. Utilization of waste feedstocks, such as used oils, for conversion to biofuels using first generation technologies negates the problems with virgin feedstocks and has future potential.

1.2.2   Second Generation Biofuels

Biofuels which are considered "second generation" come from lignocellulosic feedstocks. This plant biomass is composed of lignin and cellulose molecules, both of which are energy-dense and capable of producing liquid fuels. Several methods of conversion to fuel are currently being developed, including gasification and Fischer-Tropsch (F-T) synthesis, pyrolysis, and mechanical extraction methods. The main advantages to these second generation biofuels are that they do not compete with food feedstocks and have a better carbon balance than first generation biofuels, so long as

deforestation does not result. Another potential advantage is projected cost reduction once some of these methods are developed at a commercial scale [30, 33].

1.2.3   Third Generation Biofuels and Beyond

Algae oils are the sole feedstock for "third generation biofuels". These oils are especially interesting due to their potential volumetric yield of renewable fuels. Algae are the world's fastest growing plant and can be composed of approximately 50% oils on a dry weight basis [34]. These oils have the potential to make excellent feedstocks for biodiesel or other green diesel fuels. The yield of oil per land use has the potential to be at least 10 times better than the best crop used today [35]. However, algae oil production is still a developing technology. Currently, yields are small and concerns about energy and water usage exist. Political debate surrounding the funding of algae research has taken center-stage recently [36]. If algae oils are to be an energy source of the future, much more research and optimization is needed.

As more biofuel technologies are developed, more generations of biofuels are defined. "Fourth generation" is a recently-created term used for a biofuel development that does not fit into one of the first three generations. Production technologies such as production of biogasoline from oil and biodiesel have been referred to as "fourth generation", as have technologies in which microbes convert carbon dioxide directly into useable fuels [33, 37]. In coming years, this vague definition of fourth generation biofuels should become clearer.

1.3 Overview of Fat Molecules

Fats are biologically produced compounds whose main function is energy storage. They are a subset of the general lipid classification, which also includes steroids, phospholipids, and terpenes [38]. The high energy content of these molecules makes them natural feedstocks for conversion to biofuels.

1.3.1 Free Fatty Acids (FFA's)

Fatty acids are characterized by two functional groups: a polar carboxyl group, consisting of one carbon atom single bonded to a hydroxyl group and double bonded to an oxygen atom, and a non-polar, straight-chain, aliphatic tail, composed of carbon and hydrogen. The carboxyl group qualifies fatty acids as carboxylic acids. The tail is where much of the energy in the molecule is stored. Free fatty acids (FFA's) are fatty acid molecules that are not bonded to anything else. An example of an FFA molecular structure can be seen in Figure 1.9.
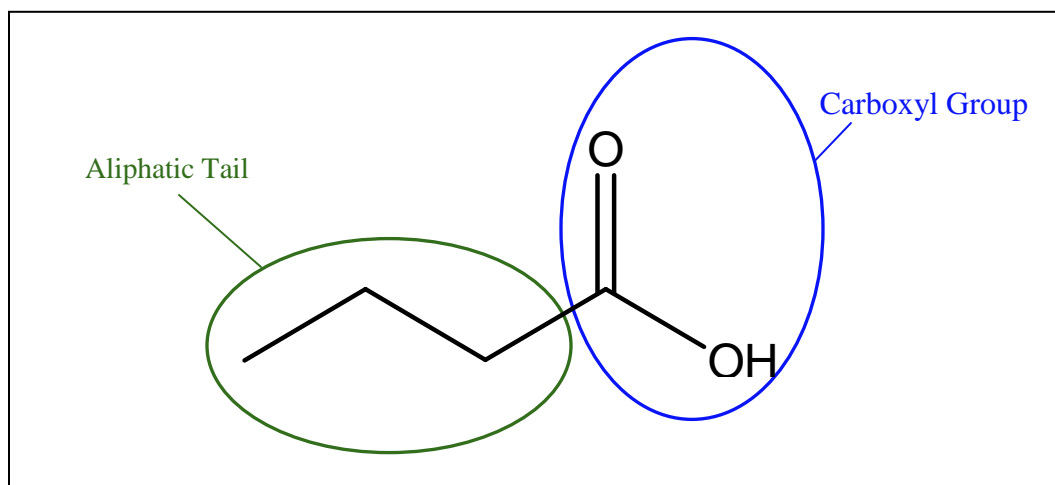
Figure 1.9: The molecular structure of butyric acid, an example of a free fatty acid (FFA)

1.3.1.1   Structure and Bonding

The molecular structure of the aliphatic tail in fatty acids dictates their properties.

Most naturally occurring fatty acids have an even number of carbon atoms in their tails

because living organisms assemble these molecules with building blocks consisting of

two carbons each [39]. Short-chain fatty acids with less than eight carbons are relatively

hydrophilic in nature, as the carboxyl group has a greater effect. Medium- (10-14

carbons) and long-chain (>16 carbons) fatty acids (LCFA's) have more hydrophobic

properties, as the properties of the aliphatic tail are more pronounced [40]. Although all

categories of fatty acids can occur naturally, LCFA's are the most naturally abundant and

have the highest energy content for potential conversion to biofuels.

Saturation is an important property for determination of physical properties of

fatty acids. Saturated acids have all single carbon-carbon bonds in the aliphatic tail.

Those with one or more double- or triple-bonds are classified as unsaturated. Double

bonds can either be *cis* or *trans* to each other, an important distinction which yields very

different properties. *Cis*-oriented bonds tend to impede molecules from aligning, causing

them to remain liquid at lower temperatures. Interesting trends are observed in the

molecules listed in Table 1.2. The melting point drops drastically from the 2C to 4C fatty

acid, and then steadily increases as the aliphatic tail grows. This can be explained with

the dominant hydrogen bonding interactions when only two carbons are present in the

molecule, causing it to stay solid at higher temperatures [41]. Once this effect diminishes

with longer carbon chains, melting points are based on molecular size and cis-double

bonds. A common method of identifying fatty acids is through two numbers, separated

by a colon. The first indicates the number of carbon atoms in the chain, while the second

is the number of unsaturated bonds [39].

1.3.1.2 Acidity

General acidity of fatty acids can be explained through resonance stability of the

conjugate base of the fatty acid. Once the acidic proton is removed from the carboxyl

group, the negative charge in the carboxylate ion is shared between the two oxygen atoms

[42]. A more stable resonance structure in the conjugate ion will make that neutral fatty

acid more acidic.
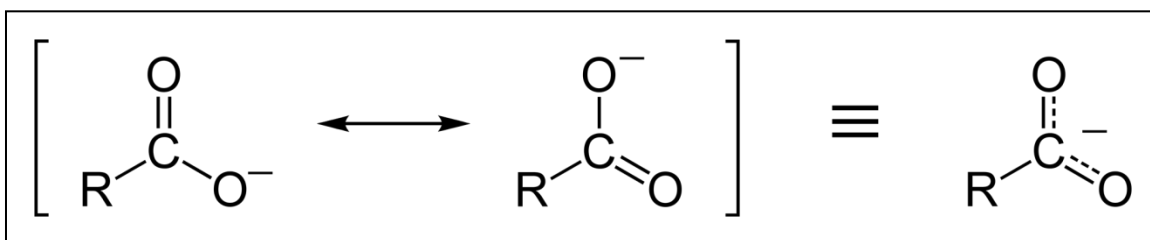
Figure 1.10: Resonance structures of the carboxylate ion, causing stability in the

conjugate base of fatty acids

Acidity is commonly measured by pK_a, with lower pK_a values signifying greater

acidity. These values for fatty acids show some trends, as demonstrated by the pKa

values in Table 1.2. As carbon chain length increases, pK_a also increases, thus

decreasing the acidity due to attractive van der Waals forces in the hydrocarbon chain

decreasing molecular separation and blocking the attack of a hydroxide group on the

acidic proton [43]. When comparing the saturated C18 fatty acid to the monounsaturated

and polyunsaturated C18 fatty acids, the pK_a decreases and acidity increases as the

molecule becomes more unsaturated. This is because *cis* double bonds prevent the molecules from stacking together, making them more soluble in polar solvents and increasing the accessibility of the acidic proton for a reacting hydroxide group.
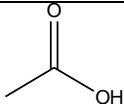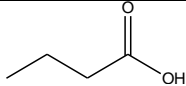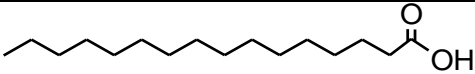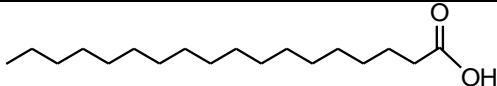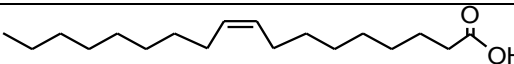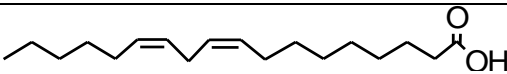
Common Name	C : D	MP (K)	pK$_a$	Structure
Acetic Acid	(2:0)	290	4.76	
Butyric Acid	(4:0)	268	4.82	
Palmitic Acid	(16:0)	335	6.4	
Stearic Acid	(18:0)	341	10.15[2]	
Oleic Acid	cis-(18:1)	289	9.85[2]	
Linoleic Acid	cis-(18:2)	266	9.24[2]	

Table 1.2: Comparison of properties for some common fatty acids [44, 45]

1.3.2   *Triglycerides*

Naturally, most fatty acids are not "free". They are usually attached to some kind of chain or backbone with other fatty acid molecules. The most common chain structure is a triglyceride, which consists of three fatty acid molecules attached to a glycerol chain.

One triglyceride molecule can have three very different fatty acids, in both length and bonding structure [39]. A typical triglyceride molecule is shown in Figure 1.11.
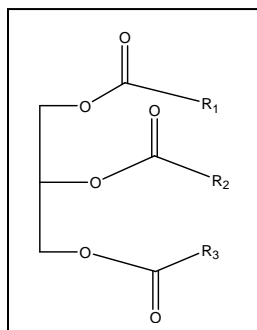
Figure 1.11: A typical triglyceride structure, where R_1, R_2, and R_3 can represent identical or different structures of the aliphatic tails

1.3.2.1 Composition of Common Oils

Oils vary greatly in their compositions. Oleic acid (18:1) is the most common naturally occurring fatty acid, but many oils and fats have greater compositions of saturated or polyunsaturated fatty acids, as illustrated in Table 1.3 below. The composition of the fats and oils determine their physical properties, as well as their health properties for human consumption [46].

Vegetable Oil	Fatty Acid					
	16:0	18:0	20:0	18:1	18:2	18:3
Soybean	11.75	3.15	0	23.26	55.53	6.31
Rapeseed	3.49	0.85	0	64.40	22.30	8.23
Sunflower	6.08	3.26	0	16.93	73.73	0
Corn	11.67	1.85	0.24	25.16	60.60	0.48

Table 1.3: Chemical composition of common oils, by percentage [47]

1.3.3   Reactivity

Several reactions involving triglycerides and FFA's are especially important for this research project. Due to the weak acidity of these molecules, reactions of FFA's with basic compounds produce salts (also called soaps) and water through the saponification reaction shown in Figure 1.12 [48]. The salts produced have ionic characteristics, making them much different than the fatty acid molecules.
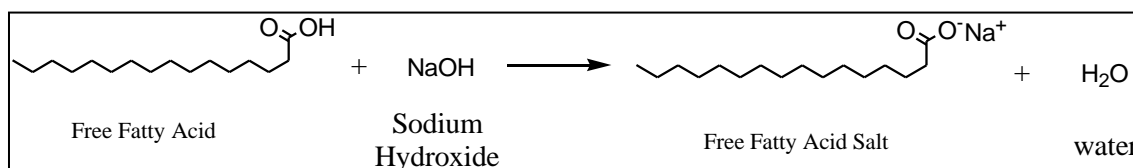
Figure 1.12: Reaction of an FFA and a strong base to produce a salt and water

A triglyceride molecule can also be converted into free fatty acids or salts through a hydrolysis reaction. Three molecules of water react with one triglyceride, catalyzed by either an acid or base, to form three FFA's and one glycerol molecule, as shown in Figure 1.13. If a base is present, these FFA's will be converted into salts through the reaction pathway in Figure 1.12.
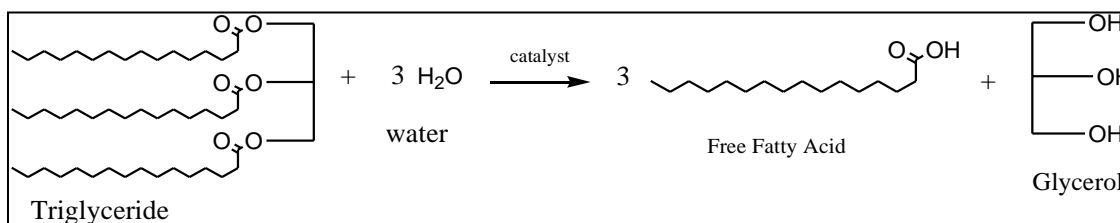
Figure 1.13: Hydrolysis reaction of a triglyceride

Commercially, the most important reaction of fats is the production of biodiesel. The transesterification reaction between a triglyceride and alcohol in the presence of a

basic catalyst produces three molecules of fatty acid methyl esters (FAME's, also known as biodiesel) and one glycerol molecule, as shown in Figure 1.14 [47]. During biodiesel production it is imperative that the presence of both water and FFA's is minimized, as both will lead to salt or soap formation. The presence of soap is undesirable in any fuel product.
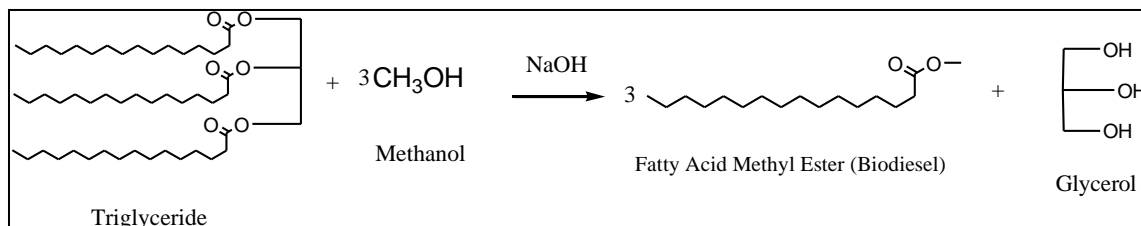
Figure 1.14: Transesterification of triglyceride to produce biodiesel

1.4 Electrochemistry Overview

Two basic categories of electrochemistry exist. The first, which includes batteries and fuel cells, involves the use of chemical reactions for the production of electric power. The second is termed electrolysis, in which electric power is used to drive chemical reactions. Both categories require a reduction-oxidation, or "redox" paired reaction with two electrodes, which can be composed of the same or different material. One electrode is termed the "anode", where an oxidation reaction occurs, and the other is the "cathode", where the balancing reduction reaction takes place.

An electrochemical cell requires both an electric and ionic conductor. In the case of electrolysis, the electric conductor is usually a metal wire hooked to some sort of external electricity source, allowing electrons to flow between the anode and cathode with minimum resistance. The ionic conductor is usually a solution with ions in it, also known

as an electrolyte. This electrolyte conducts current through chemical reactions of these ions at the electrode surfaces, which inherently provides some resistance in the circuit due to mass transfer and reaction kinetics limitations. An external voltage (also called potential) is necessary to drive reactions in electrolysis, just like activation energy is necessary to drive most chemical reactions.

Organic electrochemistry is a small subset of the total electrochemical field. Nearly all commercial-level electrochemistry is inorganic and aqueous in industries such as metal plating and chloralkali processing. Organic electrochemistry usually involves non-aqueous electrolytes and higher voltages. Despite inorganic electrochemistry' dominance in the field, a growing interest is being taken in the organic side, as demonstrated by the exponential increase in publications over recent years in Figure 1.15 [49].
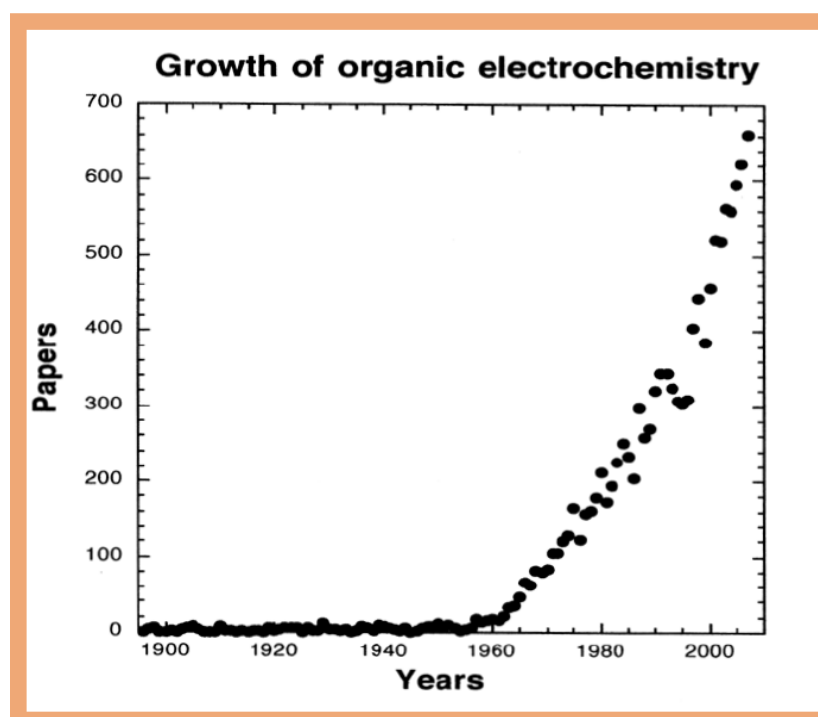
Figure 1.15: Publications per year in organic electrochemistry [48]

1.5 Project Objectives

The primary objective of this thesis is to understand and optimize the non-Kolbe electrolysis of free fatty acids (FFA's) via Hofer-Moest decarboxylation. This project is split into two separate categories of research: the organic chemistry of the reaction taking place and the engineering of the electrochemical reactor and fuel product associated with the reaction. Together, these two categories paint an interesting picture of how this process could potentially be used for the creation of a renewable diesel fuel, as well as other energy-related products.

As with all biofuels engineering, the other objectives of this project are to optimize the economic efficiency of the process and fuel quality of the product, while maximizing the production rate. The economic efficiency on a lab scale is optimized by comparing the electrical energy input to the heat produced when combusting the fuel product, directly correlated to the current efficiency of the electrolysis. The quality of the product is tested for fuel-related properties at a United States Department of Agriculture (USDA) testing laboratory. The production rate is directly related to the current measured in the electrochemical reactor. Each of these aspects of the project were better understood and theoretically optimized or maximized by varying parameters in a full factorial design of experiment (DOE). Creating recommended optimal conditions for performing this electrolysis is the final objective of this project.

1.6 Organization of Thesis

The two basic categories of objectives presented in the previous section guide the organizational structure of this thesis. Chapter 2 is based on the Hofer-Moest reaction and other organic chemistry-related aspects of this project. The molecular composition of the products from a variety of fatty acid feedstocks is examined carefully. Reaction pathways are hypothesized for each molecule in the product, and the analysis of full factorial design of experiment details which reaction parameters influence this product composition.

The engineering and fuel testing aspects of this project are the focus of Chapter 3. Diesel fuel testing results performed at the USDA/Agricultural Research Service/National Center for Agricultural Utilization Research are reported for the product generated from non-Kolbe electrolysis of a technical oleic acid feedstock. Various reactor design parameters are explored to optimize the product and maximize the production rate.

Chapter 4 presents some conclusions based on this research work. The feasibility of using alternative feedstocks is discussed. Future recommendations are presented with the goal of pushing this project forward.

1.7 References

[1] Tucker, C. (2012). Health concerns of 'fracking' drawing increasing attention: EPA conducting studies on health effects, The Nation's Health, 42, 1-14.

[2] Kerr, R.A. (2011). Peak oil production may already be here, Science, 331, 1510-1511.

[3] Shafiee, S.; Topal, E. (2009). When will fossil fuel reserves be diminished?, Energy Policy, 37, 181-189.

[4] Mathews, J.; (2008). Carbon-negative biofuels, Energy Policy, 36, 940-945.

[5] Marcus, A.; (1999). Diesel Fuel Basics, PassageMaker Magazine, Fall 1999, 1-6.

[6] Zumdahl, S. S.; (2007). Chemical Principles: 6th edition, 616-617.

[7] Western Oregon University. Energy from fossil fuels, Online Lecture, http://www.wou.edu/las/physci/GS361/Energy_From_Fossil_Fuels.htm

[8] Eberhardt, J.J. (2002). Fuels for the Future for Cars and Trucks. Diesel Engine Emissions Reduction (DEER) Workshop, 1-25.

[9] Demirbas, A. (2009). Political, economic, and environmental impact of biofuels: A review, Applied Energy, 86, S108-S117.

[10] Burri, J.; Crockett, R.; Hany, R.; Rentsch, D. (2004). Gasoline composition determined by ^{1}H NMR spectroscopy, Fuel, 83, 187-193.

[11] Ghosh, P.; Hickey, K.; Jaffe, S. (2006). Development of a detailed gasoline composition-based octane model, Ind. Eng. Chem. Res., 45, 337-345.

[12] Ophardt, C. E. (2003). What is gasoline?, Virtual Chembook – Elmhurst College, http://www.elmhurst.edu/~chm/vchembook/514gasoline.html

[13] American Society for Testing and Materials. (1989). ASTM Method D2699: Knock characteristics of motor fuels by the research method.

[14] American Society for Testing and Materials. (1989). ASTM Method D2700: Knock characteristics of motor fuels by the motor method.

[15] Yang, H.; Ring, Z.; Briker, Y.; McLean, N.; Friesen, W.; Fairbridge, C. (2002). Neural network prediction of cetane number and density of diesel fuel from its chemical composition determined by LC and GC-MS, Fuel, 81, 65-74.

[16] American Society for Testing and Materials. (2012). ASTM Method D975-11b: Standard specification for diesel fuel oils.

[17] Santana, R.C.; Phuong, T. D.; Santikunaporn, M.; Alvarez, W. E.; Taylor, J. D.; Sughrue, E. L.; Resasco, D. E.; (2006). Evaluation of different reaction strategies for the improvement of cetane number in diesel fuels. Fuel, 85, 643-656.

[18] American Society for Testing and Materials. (2010). ASTM Method D613-10a: Standard test method for cetane number of diesel fuel oil.

[19] Liang, F.; Lu, M.; Keener, T. C.; Liu, Z.; Khang, S. (2005). The organic composition of diesel particulate matter, diesel fuel and engine oil of a non-road diesel generator, J. Environ. Monit., 7, 983-988.

[20] Ott, L. S.; Bruno, T. J. (2008). Variability of biodiesel fuel and comparison to petroleum-derived diesel fuel: application of a composition and enthalpy explicit distillation curve method, Energy & Fuels, 22, 2861-2868.

[21] U.S. Energy Information Administration. (March 2012). Table 3.2: Refinery and blender net inputs and net production, U.S. Department of Energy.

[22] U.S. Energy Information Administration. (March 2011). World liquids consumptions by region, Annual Energy Outlook 2011, U.S. Department of Energy.

[23] U.S. Energy Information Administration. (October 2011). Table 5.24: Retail motor gasoline and on-highway diesel prices, 1949-2010, Annual Energy Outlook 2011, U.S. Department of Energy.

[24] U.S. Energy Information Administration. (2012). Annual Energy Outlook 2012 Early Release Overview, U.S. Department of Energy.

[25] Friedlingstein, P.; Houghton, R. A.; Marland, G.; Hackler, J.; Boden, T.A.; Conway, T. J.; Canadell, J.G.; Raupach, M. R.; Cials, P.; Le Quere, C. (2010). Update on CO_2 emissions, Nature Geoscience, 3, 811-812.

[26] U.S. Energy Information Administration. (2011). Chapter 8: Energy related carbon dioxide emissions, International Energy Outlook 2011, U.S. Department of Energy.

[27] Johnson, E. (2009). Goodbye to carbon neutral: Getting biomass footprints right, Environmental Impact Assessment Review, 29, 165-168.

[28] U.S. Energy Information Administration. (April 2011). Table C1: Estimated consumption of vehicle fuels in the United States, by fuel type, 2005-2009, Alternatives to Traditional Transportation Fuels, U.S. Department of Energy.

[29] United States Environmental Protection Agency. (December 2011). EPA finalizes 2012 renewable fuel standards, EPA-420-F-11-004, 1-3.

[30] Naik, S. N.; Goud, V. V.; Rout, P. K.; Dalai, A. K. (2010). Production of first and second generation biofuels: A comprehensive review, Renew. Sust. Energ. Rev., 14, 578-597.

[31] Goldemberg, J.; Guardabassi, P. (2009). Are biofuels a feasible option?, Energy Policy, 37, 10-14.

[32] Murphy, D. J.; Hall, C. A.; Powers, B. (2011). New perspectives on the energy return on investment (EROI) of corn ethanol, Environ. Dev. Sustain., 13, 179-202.

[33] Demirbas, M. F. (2009). Biorefineries for biofuel upgrading: A critical review, Applied Energy, 86, S151-S161.

[34] Chen, Y.; Wu, Q. (2011). Chapter 17: Production of biodiesel from algal biomass: Current perspectives and future, Biofuels: Alternative Feedstocks and Conversion Processes, 399-413.

[35] Demirbas, A; Demirbas, M. F. (2011). Importance of algae oil as a source of biodiesel, Energy Conversion and Management, 52, 163-170.

[36] Dechert, S. (March 2012). Algae: Barack and Newt square off, Examiner.com, http://www.examiner.com/renewable-energy-in-houston/algae-barack-and-newt-square-off

[37] Lu, J.; Sheanhan, C.; Fu, P. (2011). Metabolic engineering of algae for fourth generation biofuels production, Energy Environ. Sci., 4, 2451-2466.

[38] Zamora, A. (2012). Fats, oils, fatty acids, triglycerides, Scientific Psychic®, http://www.scientificpsychic.com/fitness/fattyacids.html

[39] Doonan, S. (1969). Biological formation and reactions of the –COOH and –COOR groups, *The Chemistry of Carboxylic Acids and Esters (Patai, S.),* 923-1056.

[40] Fernandex-Garcia, E.; Carbonell, M.; Calzada, J.; Nunez, M. (2006). Seasonal variation of the free fatty acids contents of Spanish ovine milk cheeses protected by a designation of origin: A comparative study, International Dairy Journal, 16, 252-261.

[41] Eberson, L. (1969). Acidity and hydrogen bonding of carboxyl groups, *The Chemistry of Carboxylic Acids and Esters (Patai, S.),* 211-294.

[42] Siggel, M. R. F.; Streitwieser, Jr., A.; Thomas, T. D. (1988). The role of resonance and inductive effects in the acidity of carboxylic acids, J. Am. Chem. Soc., 110, 8022-8028.

[43] Kanicky, J. R.; Pontatowski, A. F.; Mehta, N. R.; Shah, D. O. (2000). Cooperativity among molecules at interfaces in relation to various technological processes: effect of chain lengths on the pKa of fatty acid salt solutions, 1, 172-177.

[43] NIST Chemistry WebBook. (2011). NIST Standard Reference Database Number 69. http://webbook.nist.gov/chemistry/

[44] Kanicky, J. R.; Shah, D. O. (2002). Effect of degree, type, and position of unsaturation on the pK_a of long-chain fatty acids, Journal of Colloid and Interface Science, 256, 201-207.

[45] Williams, C. M. (2000). Dietary fatty acids and human health, Ann. Zootech., 49, 165-180.

[46] Ali, Y.; Hanna, M. A. (1994). Alternative diesel fuels from vegetable oils, Bioresource Technology, 50, 153-163.

[47] Ma, T. S. (1969). Analysis of carboxylic acids and esters, *The Chemistry of Carboxylic Acids and Esters (Patai, S.),* 892.

[48] Fry, A. J. (2009). Organic electrochemistry as a community, The Electrochemical Society Interface, The 2008 Manuel Baizer Award Address, 28-33.

Chapter 2 – Organic Electrochemistry and Characterization of Products

Products created during non-Kolbe electrolysis of long-chain fatty acids are characterized in this chapter. The anodic oxidation of pure free fatty acid (FFA) feedstocks on a graphite surface led to the formation of carbon dioxide via decarboxylation and the presence of a carbocation intermediate. The resulting Hofer-Moest reaction with this intermediate produced a combination of alkenes and ethers. Products of the Hofer-Moest reaction in methanol of oleic, palmitic, and myristic acid were first characterized via Gas Chromatography/Mass Spectroscopy (GC/MS) analysis. Products from the non-Kolbe electrolyses of oleic acid in methanol and ethanol were then compared. Finally, a full factorial design of experiment was carried out to study the effect of four parameters (ion concentration, temperature, pH, and salt type) on product yields and ratios.

2.1 Introduction

As the global search for new renewable energy sources intensifies, new methods of synthesizing fuels are being further researched. Organic electrochemistry is a field which could provide a pathway for producing a drop-in replacement for petroleum diesel fuel. Some advantages of this fuel synthesis method include mild reaction conditions, inexpensive materials of construction, and the relatively stable cost of electricity [1]. Free fatty acids (FFA's) readily form salts when reacted with strong bases, as shown in Figure 1.12. Kolbe electrolysis of these salts can occur at high current densities, high ion concentrations, and on smooth electrode surfaces, such as platinum. The anodic decarboxylation of the salts produces carbon dioxide and an intermediate radical through a one-electron transfer. Two of these radicals then dimerize, creating a "coupled" hydrocarbon product of twice the length of the carbon chain. In the case of long-chain fatty acids (LCFA's), this length would produce solid waxes rather than liquid fuels [2].

In contrast, non-Kolbe electrolysis (also known as abnormal Kolbe electrolysis) on graphite electrodes at low current densities promotes a Hofer-Moest two-electron reaction takes place whereby LCFA salts can be decarboxylated [2-4], resulting in a liquid hydrocarbon fuel with one additional double bond. The salts must be ionized in a non-aqueous solvent, usually methanol, to form an electrolyte, although non-Kolbe electrolysis in other solvents such as ethanol and DMF has also been observed [5]. Hofer-Moest products from alcoholic electrolytes also contain alcohols, ethers, and esters. These products contain an increased heating value and more desirable fuel properties than biodiesel, creating a natural possibility for a green diesel fuel replacement.

Straight-chain FFA's with 12-20 carbons in the aliphatic chain are of particular interest as a potential fuel or in other hydrocarbon synthesis applications because of their natural abundance. Many common fatty feedstocks, such as soybean oil and olive oil, are composed of exclusively fatty acids in this range. Oleic acid, the monounsaturated 18-carbon fatty acid, is the most widespread in nature [6]. In this study, three FFA's of natural abundance were studied: oleic acid (18:1), palmitic acid (16:0), and myristic acid (14:0). This allowed for characterization of Hofer-Moest products based on both saturation and carbon-chain length of the fatty acid feedstock.

Naturally produced fatty acids are usually in the triglyceride form, with three FFA's connected with a glycerol backbone. These triglycerides can easily be transesterified, catalyzed by a base such as sodium hydroxide, into esters during biodiesel production, as shown in Figure 1.14. However, if the feedstock was used in high temperature applications such as cooking, the glycerol backbone can sometimes break, yielding high FFA concentrations [6]. High FFA concentrations are typical in brown grease wastes and the expanding field of algae oil production. Base-catalyzed transesterification of triglycerides for biodiesel production is severely hindered when using feedstocks with high FFA concentrations. Triglycerides can also easily be broken into FFA salts through hydrolysis with an aqueous base, forming glycerol as a byproduct, as shown in Figure 1.13. When water is present in biodiesel feedstocks, this salt-producing mechanism leads to major problems with biodiesel production. Non-Kolbe electrolysis could be an alternative for fuel conversion for feedstocks with high FFA or water concentrations.

2.1.1 Hofer-Moest Reaction and Non-Kolbe Electrolysis

As noted in previous studies, products created from Hofer-Moest decarboxylation usually include alkenes, alcohols, and esters [2-4]. The range of products provides evidence of the brief existence of a carbenium ion intermediate after the decarboxylation and removal of two electrons, which contrasts with Kolbe electrolysis where only one electron is withdrawn during the decarboxylation, and dimers are produced through the reaction of two radicals [2]. Kolbe electrolysis occurs at high current densities, in electrolytes with high ion concentrations, and at smooth anode surfaces, such as platinum [2]. Non-Kolbe electrolysis is preferred at lower current densities and ion concentrations, and at porous anode surfaces, such as graphite.

In this chapter, insight into the products created in a simple electrochemical reactor through non-Kolbe electrolysis is provided. The pattern of GC/MS peaks created by Hofer-Moest products of each fatty acid is first analyzed. Reaction pathways for the creation of these products during the Hofer-Moest decarboxylation are concluded by comparing products created in a methanolic electrolyte against products created in an ethanolic electrolyte. Finally, a full factorial design of experiment (DOE) is performed to determine the effect of increasing temperature, pH, concentration, and changing the alkali metal cation present in solution.

2.2 Experimental

2.2.1   Reactor and Electrode Pack

A 250-mL electrochemical reactor was assembled to perform experiments. A glass jar was fitted with a rubber stopper and condenser to minimize solvent losses. An undivided "electrode pack" was assembled with six graphite plates, each 9 cm x 4 cm, held together with nylon threads and bolts, with 3 mm plastic spacers between each plate. This spacing allowed for fluid movement between plates with minimal resistive heating losses. No membrane or separation of any sort was used between each anode and cathode. The plates created five cells in series where redox coupled reactions could occur. The end graphite slabs on each side of the electrode pack were connected to a direct current (DC) potentiostatic source, set at 20 V or 4 V/cell. This setup caused the spaces between graphite plates to act as resistors in series. The cell potential was found to drive the non-Kolbe electrolysis and decarboxylation of carboxylic acids in this system at a reasonable rate. A combined magnetic stirring/hot plate allowed for constant mixing of the solution and temperature control for a water bath surrounding the reactor.
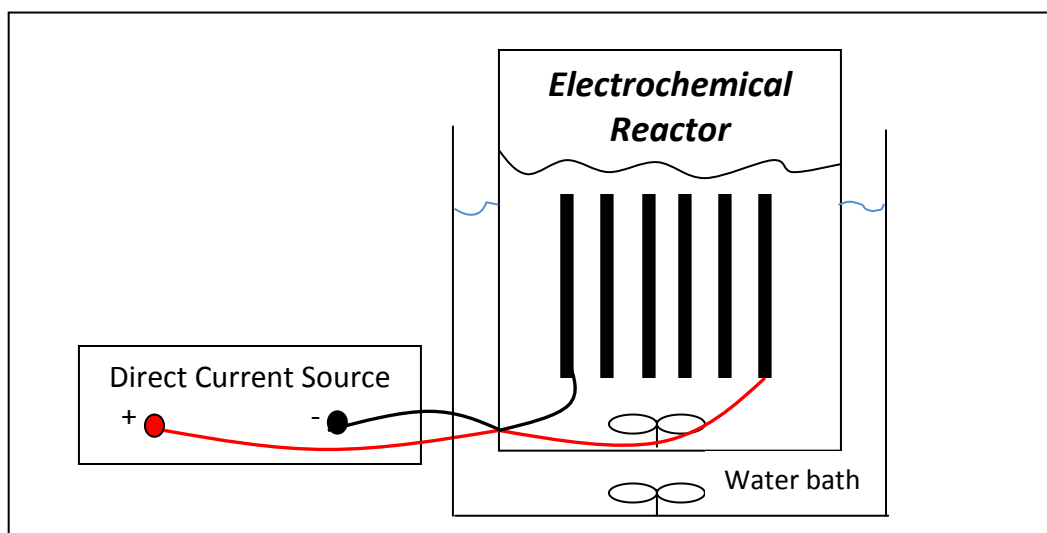
Figure 2.1: Diagram of electrochemical set-up

2.2.2. Preparation of Electrolyte and Reaction Conditions

An electrolyte was created by dissolving 0.10 M caustic (sodium hydroxide, unless otherwise notes) into 250 mL of methanol or ethanol, creating small concentrations of hydroxide, methoxide or ethoxide, and water through the following equilibrium reactions:

$$CH_3OH + OH^- \rightleftharpoons CH_3O^- + H_2O$$

$$CH_3CH_2OH + OH^- \rightleftharpoons CH_3CH_2O^- + H_2O$$
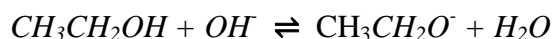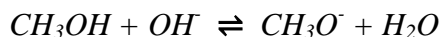
An equimolar amount of free fatty acids (FFA's) was then added and saponified through the following set of reactions:

$$R\text{-}COOH + OH^- \rightarrow H_2O + R\text{-}COO^-$$

$$R\text{-}COOH + R'O^- \rightarrow R'OH + R\text{-}COO^-$$
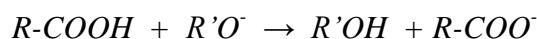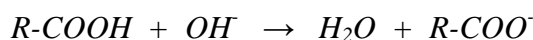
In this set of experiments, R symbolizes an aliphatic hydrocarbon chain of between 13 and 17 carbons and R' represents either a methyl or ethyl group, depending on solvent. Electrolytes with oleic acid, palmitic acid, and myristic acid were all prepared in methanol, with an additional ethanolic electrolyte prepared with oleic acid. The final concentrations of ions in the alcoholic electrolyte were approximately 0.10 M Na^+, 0.10 M $R\text{-}COO^-$, 0.10 M H_2O, and very small amounts of methoxide (CH_2O^-) or ethoxide ($CH_3CH_2O^-$) with negligible hydroxide (OH^-).

Each electrolyte was then added separately to the clean reactor with the graphite electrode pack. Each solution was constantly stirred and kept at approximately 20°C. The 20 V DC current (4.0 V/cell) was then applied for 20 minutes, with current being recorded. Bubbles of gas from both the anode and cathode were noted, evidencing the

formation of carbon dioxide on the anode after decarboxylation and hydrogen gas on the cathode as a balancing reduction reaction.

2.2.3 Analytical Methods

A 3 mL aliquot of the electrolyte after each electrolysis was added to a 3 mL sample of pure hexane. Partitioning of the product led to the relatively non-polar products of the Hofer-Moest reaction preferring the hexane phase. Two microliters of this hexane phase were then diluted and saved for Gas Chromatography/Mass Spectroscopy (GC/MS) analysis.

The GC/MS analysis was performed on a 6890 Series GC system with a 5973 Network MSD from Agilent (Santa Clara, CA). The column used was a 0.25 micron HP-5MS, 30 m x 0.250 mm, also from Agilent. Electron ionization (EI) fragmented molecules for identification and analysis with helium carrier gas at 70 eV. The temperature program held at 50°C for 5 minutes with a 4.20 minute solvent delay, ramped at 10°C/minute for 25 minutes to 300°C, then held at 300°C for 10 minutes. The NIST 2008 Mass Spectroscopy library helped identify fragmentation patterns. A chemical ionization (CI) was also performed with methane carrier gas to get better precision near the molecular ion in the mass spectra.

2.2.4 Full Factorial Design of Experiment (DOE)

A full factorial design of experiment was then set up to be performed with the electrolysis of palmitic acid salts. Four reaction parameters were chosen to study: temperature, ion concentration, pH, and type of alkali base used to neutralize the fatty

acid. Two levels for each parameter were chosen.   Table 2.1 summarizes the binary

levels of each parameter for experimentation. A molar excess of base was designed to

ensure that all free fatty acids were completely saponified. All experiments were

performed with methanol as a solvent. After each experiment GC/MS samples were

acquired with the previously described method.

	-	+
Base/Acid Ratio (molar)	1.10	1.30
Conc (M)	0.05	0.1
Base	NaOH	KOH
Temp (°C)	20	50

Table 2.1: Summary of lower level and higher level for each varied parameter in the full

factorial design of experiment

2.3 Results and Discussion

2.3.1 *Hofer-Moest Products from Myristic, Palmitic, and Oleic Acids*

The Hofer-Moest products from non-Kolbe electrolysis in methanol with myristic,

palmitic, and oleic acid all showed a similar pattern, as can be seen in Figures 2.2-2.4,

respectively. Nine characteristic peaks were identified in each GC/MS analysis. An

initial cluster of five primary peaks were identified as hydrocarbons in each sample, with

retention times between 14 and 15 minutes in the myristic sample, 17 and 18 minutes in

the palmitic sample, and 19 and 20 minutes in the oleic sample. An additional peak was

noted in the hydrocarbon range of the oleic acid product. In each case, the largest peak in

that cluster was positively identified as the 1-alkene product through comparison to the

NIST 2008 MS Library. Due to the scarcity of the other alkene molecules, these other peaks did not yield positive confirmation of their identity from their fragmentation patterns. The second, third, and fourth peaks fit the patterns of other constitutional isomers of the alkene, possibly with double bonds in the 2- or 3- position. The fifth peak suggested another hydrocarbon, likely another alkene isomer or possibly a cyclic structure. The sixth, seventh, and eighth peaksdid not show a definitive molecular ion in their EI fragmentation patters, so a softer chemical ionization (CI) technique with a methane carrier gas was used to identify molecular ions. . The CI technique showed that all three peaks were ethers, and the EI fragmentation pattern provided clues as to which ether isomer corresponded to each of the peaks. In the MS fragmentation pattern, the ion with the largest abundance, called the base peak, corresponded to the product formed from the cleavage of the C-C bond to the α-carbon from the methoxide group of the ether. Using this reasoning, the sixth peak in the GC was hypothesized to be a secondary ether with the methoxide group attached to the third carbon in the chain, the seventh peak was hypothesized to be the secondary ether with the functional group bonded to the second carbon, and the eighth peak corresponded to the primary ether bonded to the terminal carbon. The final peak was positively identified as the methyl ester of the fatty acid. This is not a product of the electrochemistry of this reaction, but rather the result of the esterification of the FFA and alcohol before saponification. MS results for each peak in the palmitic and oleic samples can be found in the Appendix.
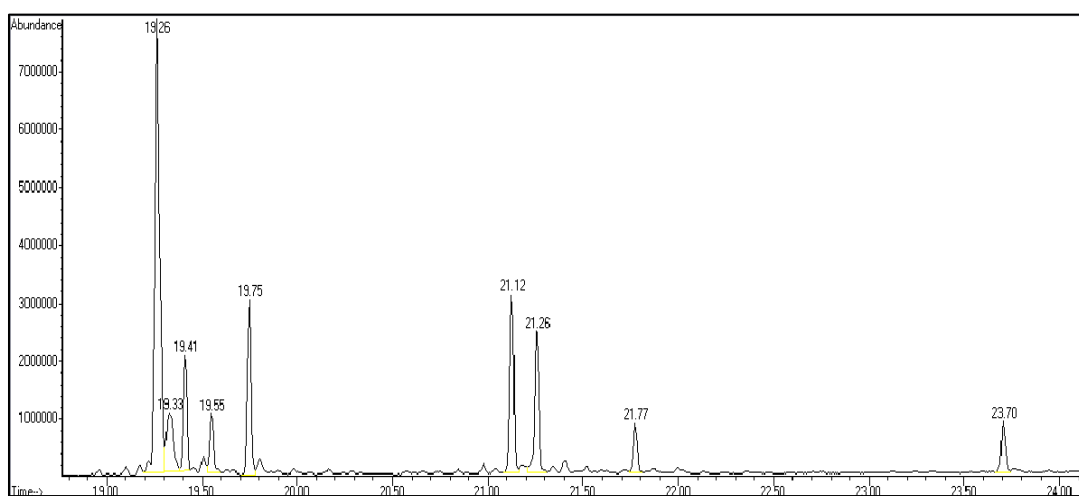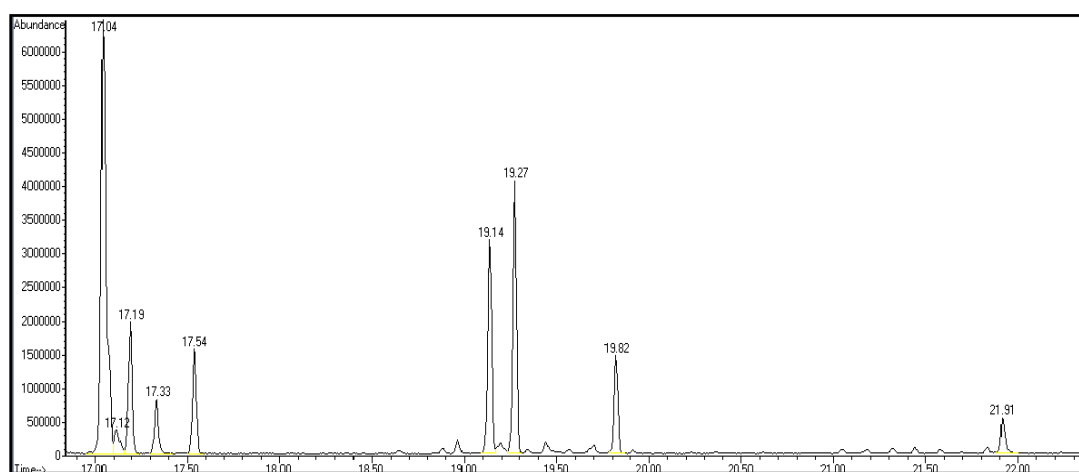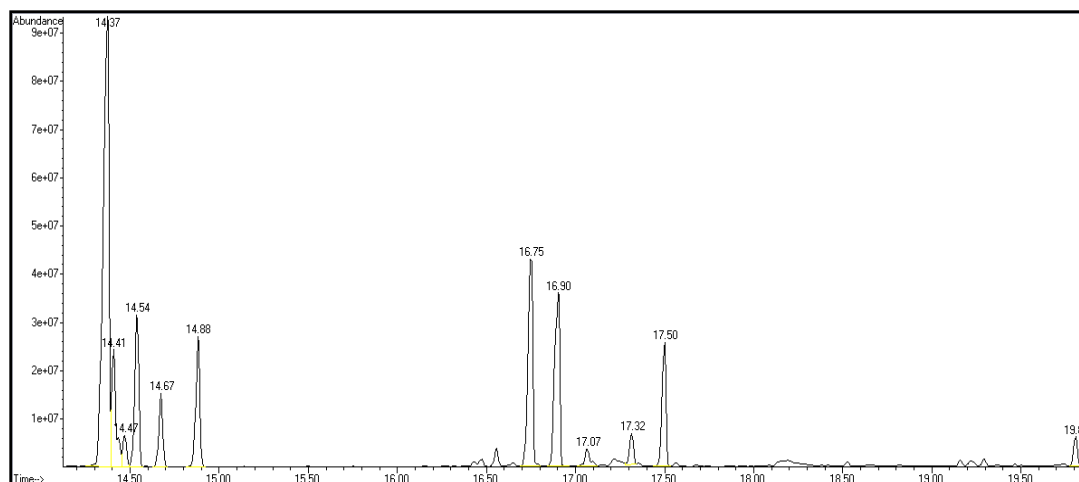
Figure 2.2-2.4: GC/MS results of Hofer-Moest products derived from myristic acid

(14:0), palmitic acid (16:0), and oleic acid (18:1) with retention times for product peaks

Although no exact quantitative methods were used with the GC results, the distribution of products in each sample was estimated by proportioning the areas of each peak [7]. Table 2.2 lists the retention time and relative distribution (by mass) based on peak area of each molecule in the products, while Table 2.3 summarizes the approximate concentration of each type of molecule in the product. The oleic acid products had the largest percentage of alkene peak areas, while the saturated fatty acid products had a greater percentage of the total peak area under the ether peaks. A possible explanation for this is that the double bond in the alkyl chain of oleic acid helped to stabilize the positive charge in the carbenium ion. This greater stability allowed for more charge displacement and a better likelihood of losing an additional proton to form an alkene. With the less stable, saturated carbenium ion, an immediate reaction was more likely to take place. This promoted the reaction between the carbenium ion and methoxide group to form an ether. Several of the possible reaction pathways for the carbenium ion of oleic acid are shown in Figure 2.5. A surprising result from this analysis is that no long-chain alcohols were formed from the reaction of a hydroxide group and the carbenium ion. A hypothesized reason for this is that the excess of methanol in the equilibrium between methanol and hydroxide pushes it towards methoxide and water, depleting the concentration of hydroxide ions, especially near neutral pH conditions.

Peak No.	Myristic		Palmitic		Oleic	
	RT	Distr	RT	Distr	RT	Distr
1	14.37	37.7%	17.04	36.2%	19.26	39.7%
2	14.41	5.7%	17.12	2.4%	19.33	7.3%
3	14.54	8.9%	17.19	8.1%	19.41	8.2%
4	14.67	4.1%	17.33	3.7%	19.55	4.6%
5	14.88	7.7%	17.54	6.9%	19.75	11.3%
6	16.75	14.0%	19.14	13.6%	21.12	11.9%
7	16.90	13.4%	19.27	17.3%	21.26	10.6%
8	17.50	7.0%	19.82	7.2%	21.77	3.3%
9	19.81	1.5%	21.91	4.6%	23.70	3.1%

Table 2.2: Summary of the nine main Hofer-Moest products detected by GC/MS from

three different fatty acids
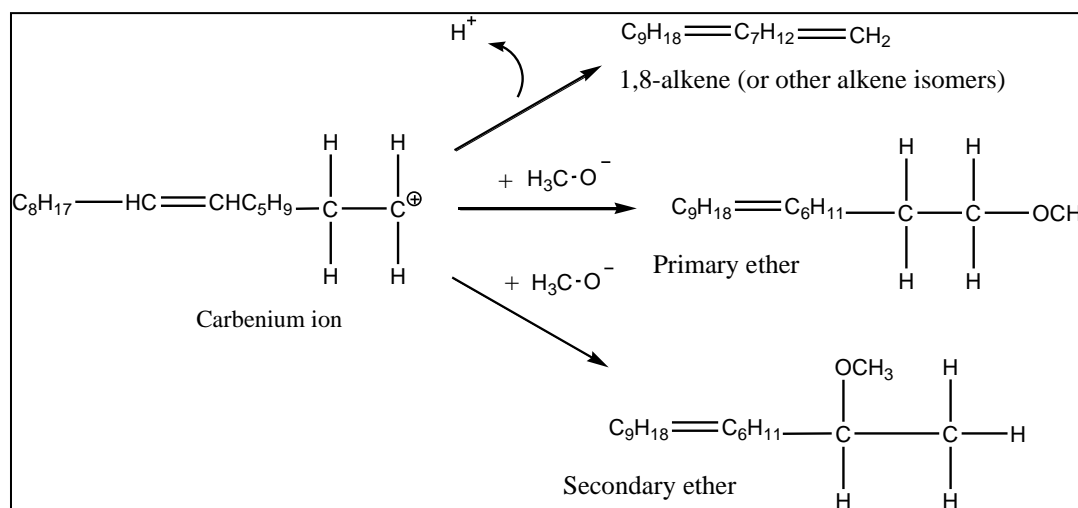
Figure 2.5: Several possible reaction pathways for the carbenium ion in the Hofer-Moest

reaction

	Myristic	Palmitic	Oleic
Hydrocarbons	64.1%	57.3%	71.1%
Ethers	34.4%	38.1%	25.8%
Methyl Esters	1.5%	4.6%	3.1%

Table 2.3: Composition of products by molecular classification based on GC/MS peak areas

2.3.2 *Effect of Solvent on Product Composition*

Products from methanol and ethanol non-Kolbe electrolyses of oleic acid provided some interesting insight into the reaction. Because the same reactor was used, traces from the methanol products showed up in the GC/MS result from the ethanol electrolysis, but they were easy to identify. A similar pattern of hydrocarbons is identified on the two GC/MS results shown in Figures 2.6 and 2.7. The middle of the spectrum is where the retention times of peaks start changing. Since an ether created in the ethanol would be an ethyl ether instead of a methyl ether, a small shift in retention times would be expected. The absence of peaks at retention times 20.56, 20.69, and 21.21 in the ethanol electrolysis shows that these products must be related to the solvent.
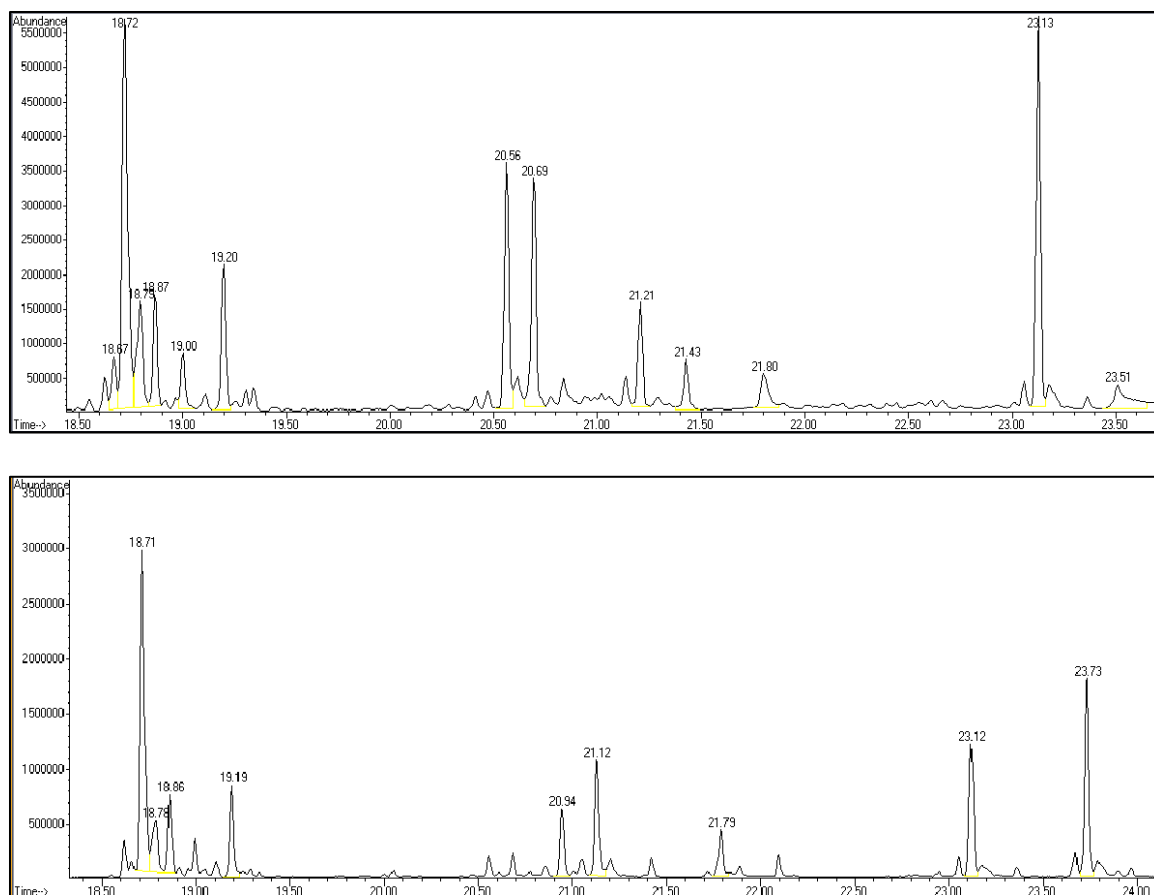
Figure 2.6-2.7: Comparison of GC/MS spectra of Hofer-Moest products from non-Kolbe

electrolysis of oleic acid in methanol (Figure 2.6) and ethanol (Figure 2.7)

2.3.3   Full Factorial Design of Experiment (DOE)

A total of 16 experiments were carried out with palmitic acid to test the binary

levels for reaction parameters outlined in Table 2.1. Eleven outputs for each of the

experiments were tested for statistical significance: each of the percentages of the nine

peaks identified in Table 2.2, plus the total peak area of all peaks and the total number of

coulombs recorded in the 20 minute electrolysis. Using the statistical software package

Minitab®, a P-value was calculated for each varying parameter's effect on each output.

A significance level (α) was set at 0.05. A P-value less than the significance level represented that a "null hypothesis" was rejected. In this case, the default for the null hypothesis was that the particular parameter being tested did not have a significant effect on the output. For this analysis, P-values of less than 0.05 represented a parameter which was concluded to have had a significant effect on that particular output when comparing that parameter's binary testing levels.

Table 2.4 shows the P-values for each reaction parameter and each output. The calculations for the separate peaks were based on the *percentage* of the area of the peak at that retention time compared to the total area of all peaks for that sample. It was not a comparison of the net areas of that particular peak between samples. Seven total P-values were less than the significance level (highlighted in red in Table 3), representing effects which needed to be further analyzed.

P-values											
			Peak Retention Times									
Parameter	*Coulombs*	*Total Area*	*17.05*	*17.12*	*17.20*	*17.33*	*17.54*	*19.14*	*19.28*	*19.82*	*21.92*
Base/Acid	0.350	0.745	0.701	0.144	0.483	0.807	0.737	0.019	0.009	0.641	0.070
Concentration	0.003	0.016	0.827	0.068	0.624	0.587	0.373	0.159	0.624	0.410	0.295
Base	0.235	0.198	0.517	0.680	0.957	0.787	0.376	0.246	0.966	0.966	0.729
Temperature	0.035	0.453	0.225	0.139	0.248	0.354	0.032	0.003	0.500	0.120	0.225

Table 2.4: P-values for outputs from full factorial DOE, with significant factors

(α > 0.95) highlighted

The 0.10 M palmitate ion concentration level had a significant effect on both the total coulombs measure (signifying greater current/electrical charge) and the total area of the sum of the nine significant peaks in the GC/MS sample. This makes sense with respect to electrochemistry fundamentals. Greater ion concentrations allow for more conductivity of electrons and more reactions at the anode and cathode surface. The greater reactivity creates more Hofer-Moest products, as detected in the GC/MS sample, so the second result made sense as well. A 50°C temperature also significantly increased conductivity. When considering surface-limiting reactions at the anode, which is believed to be the case in this electrolysis, a higher temperature would promote more diffusion of ions and products to and from the surface, thereby increasing reactivity and electrical current. A surprising result is that temperature did *not* have a significant effect on the total area of product in the GC/MS sample. A hypothesized reason for this is that an increase in side reactions, such as the oxidation of methanol or water, occurred at the higher temperature rather than Hofer-Moest product-forming decarboxylation. This result signified a drop in current efficiency at the higher temperature.

Four other significant effects were noted in the percentage of products formed. The 20°C temperature caused a greater percentage of peaks at retention times 17.54 and 19.14 minutes to form. From the previous discussion, based on MS fragmentation patterns, we hypothesized that the peak at 17.54 could be a cyclic structure of some sort, and that the peak at 19.14 was a secondary ether. The more energy in the system at the higher temperature may have caused more reactivity. The carbenium ion would have been more likely to react immediately at this higher temperature with a methoxide group,

creating a primary ether. At a lower temperature, the decreased energy could give the ion a chance to rearrange before reacting with the methoxide group.

2.4 Conclusions

In the context of using non-Kolbe electrolysis for the production of a green diesel fuel from FFA's, several important conclusions are drawn from this research. An assessment of the products created from non-Kolbe electrolysis from saturated and unsaturated long-chain free fatty acids shows that a higher percentage of hydrocarbons being produced from unsaturated feedstocks. These hydrocarbons closely resemble molecules in petroleum diesel, making them a better drop-in replacement fuel than ethers, alcohols, or esters. This means highly unsaturated fatty acid feedstocks will theoretically work better for this electrolysis in a fuel-related context than more saturated fatty acid feedstocks, in that they will have a higher composition of hydrocarbons.

The ability to tailor reaction conditions to vary the ratio of products and create a more efficient electrolysis also holds many potential advantages in fuel creation. The conclusions reached during the factorial design of experiment in this research mainly helped with identifying and explaining the conductivity and reaction pathways in this electrochemical set-up. The conclusion based on the factorial experiments is that an electrolyte which maximizes fatty acid ion concentration at a lower temperature will optimize production rate while maximizing current efficiency. The reality is that these experiments barely scratch the surface in exploration of potential reaction conditions of this electrolysis. Exploring other reaction parameters or more extreme levels for the parameters studied here could lead to important findings in tailoring the reaction to be

more efficient and produce a ratio of Hofer-Moest products which maximizes fuel

performance.

2.5   References

[1] Rifi, M.R.; Covitz, Frank H. (1974).   *Introduction to Organic Electrochemistry,*

Marcel Dekker, Inc.

[2] Schäfer, H. J. (1990).   *Top. Curr. Chem.*, *152,* 91–151.

[3] Schäfer, H. J. (2012).   *Eur. J. Lipid Sci. Technol. 114*, 2-9.

[4] Lund, Henning; Baizer, Manuel M. (1991). *Organic Electrochemistry: An

Introduction and a Guide*, Marcel Dekker, Inc.

[5] Klocke, E.; Matzeit, A.; Gockeln, M.; Schäfer, H. J. (2003). *Electroorganie

Synthesis*, *55*, *Chemische Berichte*, *126*, 1623–1630.

[6] Canakci, Mustafa. (2007).   *Bioresources Technology, 98,* 183-190.

[7] Sparkman, O.D.; Penton, Z.; Kitson, F. G. (2011). Gas chromatography and mass

spectroscopy, Academic Press, Inc.

Chapter 3–Engineering Design and Fuel Analysis

Optimization of the electrochemical system is important in determining if non-Kolbe electrolysis and the Hofer-Moest reaction can be used commercially to convert fatty acids into renewable diesel fuel. A vertically oriented graphite electrode pack in series maximizes current density as compared to one in parallel or horizontally oriented. Reversing the direction of flow of electrons by switching polarities periodically improves the electrode surface diffusion of Hofer-Moest product into the electrolyte. Spacing of 3 mm between graphite electrodes within the electrode pack provides homogeneous mixing and keeps ion concentration constant near the electrode surface, while minimizing resistive heating losses. A minimal voltage of approximately 2.5 V/cell was determined to drive the Hofer-Moest reaction of oleic acid in a methanolic electrolyte on graphite. A current efficiency of 73.9% is demonstrated when using a pure oleic acid feedstock, indicating that $0.383 of electricity is necessary to create one gallon of Hofer-Moest fuel from oleic acid, assuming average 2011 commercial electrical costs.

Fuel testing of the product is critical to determine if it would make a sufficient drop-in replacement fuel. Theproductproduced from a technical oleic acid feedstock (80% oleic acid, 20% other long-chain FFA's) showed an improvement in higher heating value (HHV), cloud point, and pour point in comparison to soybean biodiesel, while worsening the oxidative stability.

3.1 Introduction

3.1.1 Electrochemical Engineering

Electrochemistry has been researched since around 1800. Many important discoveries about quantitative measurements in this field were made by Michael Faraday in the early 19th century. Although much more is now known about electrochemistry, many quantitative methods developed by Faraday are still in use as the basis for electrochemical engineering [1,2].

The two basic types of electrochemistry outlined in Chapter 1 involve similar fundamentals and theories, but are often very different in design. Important considerations for electrochemical engineering include electrode materials, operational parameters, phase separations, reaction kinetics, and mass transport of ionic species. A general 14-step process for the design of an electrochemical system presented by Goodridge and Scott is summarized in Table 3.2 below [3].

1	Specify temperature, pressure, pH
2	Specify diaphragm (if required)
3	Prepare flow sheet
4	Analyze reaction kinetics, current efficiencies, mass transport rates
5	Perform material balance around process
6	Specify electrodes: Dependent upon overvoltages, cost, spacing, specificity of reaction, possible bipolar use

7	Specify reactor: Dependent on volumetric throughput, flow characteristics, required electrode area
8	Design reactor geometry: configuration of electrodes, orientation, flow path (parallel vs. series), etc.
9	Produce drawing of reactor
10	Perform reactor voltage balance
11	Determine power requirements
12	Perform energy balance
13	Estimate cost of reactor
14	Repeat steps for various reactor sizes, current densities, production rates

Table 3.1: Design procedures for scale-up of an electrochemical reactor

While much work has been done on optimizing inorganic electrochemical processes, organic electrochemical engineering has not been commercialized to the same degree [2]. Due to the insolubility of many organic ions in water, most organic electrochemistry must take place in a non-aqueous electrolyte, causing different issues than aqueous-based inorganic electrochemistry. Also, higher voltages are often necessary to drive organic reactions [4,5]. In this project, many of the same design considerations mentioned by Goodridge and Scott are applied in an organic electrochemical engineering application.

3.2.1 Petroleum Diesel and Biodiesel Fuel Testing

As discussed in Chapter 1, growing concerns about supply and climate change have spurred the growth of the renewable fuels market. Of special significance are "drop-in" replacement fuels, which can be used in modern engines. Biodiesel is a renewable diesel often blended with petrodiesel, but which can sometimes be used independently as a drop-in fuel. It isproduced from a transesterification reaction between a triglyceride and alcohol and traditionally composed of mono-alkyl esters (Figure 1.14). Production of other alkyl esters is also possible via reactions with alcohols like ethanol and propanol.

Besides being a renewable fuel, biodiesel has other advantages over petroleum diesel, such as better lubricity, enhanced cetane numbers, lack of sulfur, and greater biodegradability [6,7]. However, it also has several problems and concerns, namely increased NO_x emissions, poor cold flow properties, poor oxidative stability, and decreased higher heating values (HHV), leading to poor efficiency in engines [8]. Due to these problems, the American Society for Testing and Materials (ASTM) has created ASTM D6751-11b to specify minimum testing standards for pure biodiesel, B100 [9]. ASTM Standard D7467-10 defines testing standards for blended diesel fuels between 80-94% petroleum and 6-20% biodiesel (B6-B20) [10]. Several of the important standards are summarized in Table 3.2. Figure 3.1 shows a map of the continental United States from ASTM D7467-10, which defines the 10th percentile minimum ambient temperature by region. This map is used as a guide for the minimum standards for cold weather properties, such as cloud point and pour point, in each region for the blended fuel.

	Standard for B100 (ASTM D6751-11b)	Standard for B6-B20 (ASTM D7467-10)
Viscosity (mm^2/s at 40**°C**)	1.9-6.0	1.9-4.1
Flash Point (**°C**), min	130	52
Cloud Point (**°C**)	Report	Report
Cetane Number, min	47	40
Oxidation Stability (hrs), min	3	6

Table 3.2: Minimum fuel standards for biodiesel and biodiesel/petrodiesel blends

Figure 3.1: Map detailing 10th percentile minimum temperatures for use when referencing cold flow-related properties for fuel distribution

Petroleum diesel's minimum fuel standards are defined by ASTM Standard 975-11b [11]. Some of the important standards are included in Table 3.3. Diesel is separated into No. 1 grade and No. 2 grade. While No. 2 is predominantly used in warmer climates, No. 1 can offer better cold flow properties. Typically, oxidative stability is not an issue for petroleum diesel as it is for biodiesel. An induction period standard is not listed in ASTM 975-11b.

	No. 1-D	No. 2-D
Viscosity (mm^2/s at 40°C)	1.3-2.4	1.9-4.1
Flash Point (^{o}C), min	38	52
Cloud Point (^{o}C)	Refer to Figure 3.1	Refer to Figure 3.1
Cetane Number, min	40	40

Table 3.3: Fuel standards for petroleum diesel from ASTM D975-11b

3.2 Experimental

3.2.1 Lab Scale Set-up

Several electrochemical reactor designs and electrode configurations were tested. The first reactor was made from a 5 gallon plastic bucket. Six circular graphite plates were cut with a diameter of 25 cm to fit in the bucket. Holes with a diameter of 4 cm were drilled in the middle of each of the bottom five electrodes. Nylon threads were bolted down to keep the stack together, with plastic spacers separating each plate, creating five different electrochemical cells. The top plate and bottom plate had electrically connected copper wires. The total area for this electrode configuration was

478.3 cm^2 (per cell). Two holes were drilled in the bucket's bottom, at the center and several centimeters from the edge. The hole in the bottom middle was designed to fit the holes in the middle of the electrode pack. A 3-MD magnetic drive pump from the Little Giant Pump Company® was then connected to these holes with bulkhead adapters to recirculate the electrolyte at a flow rate of approximately 5 gallons/minute (18.9 L/min), pumping out of the reactor through the bottom offset hole and back in through the middle of the electrode pack. The concept was that with the top plate undrilled, the electrolyte would be forced out the space between the graphite plates with the pump. The sheer force of the fluid being forced between these tightly spaced surfaces would cleave product off the electrodes. To create as much shear as possible, very thin plastic spacers of 0.8 mm were used between plates. A diagram of the configuration is shown in Figure 3.2.
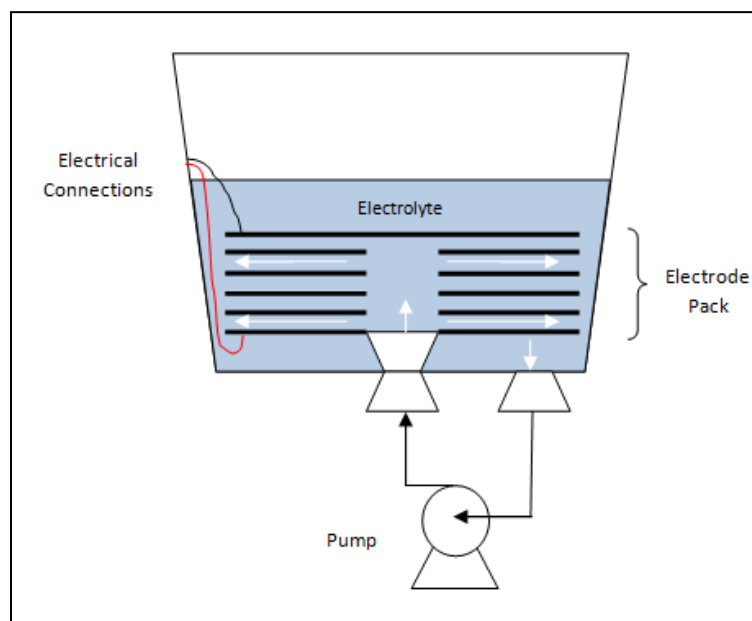

Figure 3.2: Side view of the horizontally-oriented pumping reactor design

The second and third reactors had similar designs, but with vertically oriented cells. The second, termed the "olive jar reactor", was made from a small glass jar with a capacity of 250 mL and fitted with a rubber stopper and condenser. An electrode pack of graphite rectangular plates was assembled, with electrical wires connected to the outside plates. The plates measured 9 cm x 4 cm (SA=36 cm^2). A magnetic stir bar was used to produce homogeneous mixing within the electrode pack. An external water bath was used for temperature control, allowing for experimentation at different set temperatures, whereas the bucket design did not allow for easy control of temperature. The third reactor was made out of a larger jar with a 1.5 L capacity, termed the "cookie jar reactor". A similar vertically oriented electrode pack was assembled, with rectangular electrodes measuring 8 cm x 12 cm (SA=96 cm^2). The electrodes were specially cut and each wire was run to two additional clamps so that the circuit could be set up in parallel by connecting the clamps to every other graphite plate or in series by connecting all clamps to just the outside electrode. Plastic spacers of 0.8 mm and 3 mm were tested in the olive and cookie jar configurations. A diagram representing both is shown in Figure 3.3, with a picture of the lab scale setup shown in Figure 3.4.
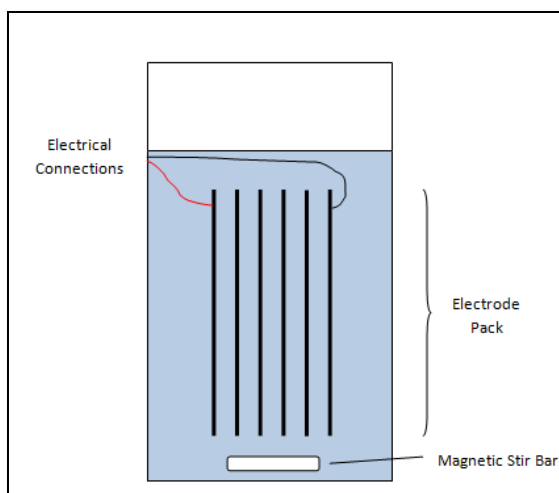
Figure 3.3: Side view of vertically-oriented glass jar reactor design
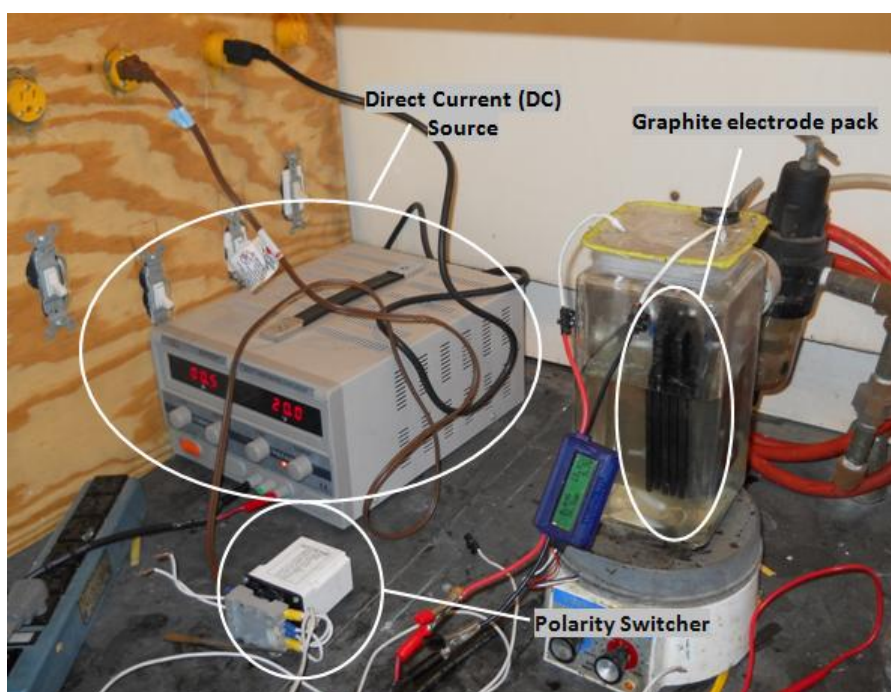

Figure 3.4: Lab scale setup with the cookie jar reactor

3.2.1.1 Direct Current (DC) Source and Polarity Switching

A device which provided direct current (DC) was necessary for reactions to take place. A Mastech HY3020E Lab Grade Switching DC Power Supply from Power Suppliers Warehouse was used for this purpose. It was able to provide either a potentiostatic source between 0 and 30 V by varying current or an amperostatic source between 0 and 20 A by varying voltage.

Since both electrodes in theelectrochemical reactor setups were graphite, the consideration about possible bipolar use in process design step 6 from Goodridge/Scott in Table 3.1was considered. A switch for automatically changing polarity direction periodically was purchased. The switch could be adjusted to toggle anywhere between fractions of a second and several hours.

3.2.2 Minimum Cell Voltage

A 0.15 M oleic acid electrolyte was produced using the same method outlined in Chapter 2. To get an idea of what cell voltage was necessary to drive the decarboxylation reaction, the electrolysis was performed in the olive jar reactor. The DC power supply was run in series at 30 minutes at 10.0 V, 12.5 V, and 15.0 V (2.0 V/cell, 2.5 V/cell, and 3.0 V/cell, respectively). After each 30 minutes, a 3 mL aliquot of electrolyte was partitioned with 3 mL of hexane to extract any product formed into the non-polar phase. The hexane phase from each of the partitioned hydrophobic phases was analyzed via GC/MS to determine when the formation of hydrocarbon and ether peaks could be observed, evidence of non-Kolbe electrolysis.

3.2.3 Current Efficiency

A fresh 0.15 M oleic acid electrolyte was again prepared with equimolar pure

oleic acid and sodium hydroxide. The cookie jar reactor was used to run the electrolysis

in a parallel setup at 4.0 V/cell, so the voltage drop remained constant in every cell.

Direct current was run in one direction for one hour while recording amperage every 15

minutes. The direction of current was then switched, and current was run the other

direction for one hour, again recording current every 15 minutes. Fresh oleic acid was

slowly added to keep the electrolyte approximately neutral (pH≈7.5). A combination of

Newton-Cotes closed integration formulas was used to numerically integrate the currents

over time (Eq. 3.1) to determine a total charge using Equation 3.1 [1,12], where Q is the

total charge in Coulombs and I is current in Amperes.

$$Q = \int I \cdot dt \qquad \qquad \textbf{[3.1]}$$

This total charge was then substituted into Faraday's Law of Electrolysis (Eq. 3.2)

to find a theoretical mass that could have been produced.

$$m_{theoretical} = \frac{Q \cdot MW}{n \cdot F} \qquad \qquad \textbf{[3.2]}$$

In this equation, MW is the average molecular weight of the products from the

electrolysis, n is the number of electrons per reaction (in the case of non-Kolbe

electrolysis, 2), and F is Faraday's constant (96,485 C/mol).

Product was then separated out from the electrolyte. An aqueous sodium

hydroxide solution was first added to the electrolyte to neutralize any FFA's. Hexane

was then used to wash the electrodes and extract any product from the electrolyte by

mixing the two phases for 15 minutes. The hexane layer was then separated and distilled,

leaving only the oleic products listed in Table 2.3. Only the hydrocarbons and ethers are

electrochemical products, so the 3.1% of methyl esters (from the product distribution for

oleic acid Hofer-Moest reactions, outlined in Table 2.3) in the product were subtracted

from the total mass of products to leave an actual mass of electrochemical

products(m_{actual}), which was then used to find current efficiency (CE) from Equation 3.3.

$$CE = \frac{m_{actual}}{m_{theoretical}}$$ **[3.3]**

3.2.3.1 Calculation of Electricity Costs

Because the electrical energy of the process converts fatty acids to Hofer-Moest

products on a molar basis rather than mass or volume, the electricity costs will be highly

dependent on feedstock composition. Higher molecular weight fatty acids will consume

less electricity during conversion per mass or volume. Pure oleic acid is used as a model

feedstock for this calculation, as its current efficiency in the process is known and it is

abundant in nature (see Table 1.3). Electrical energy was then calculated using Equation

3.4.

$$Electrical\ Energy = V \cdot Q$$ **[3.4]**

Since one volt (V) is equivalent to one joule (J) per coulomb (C), the electrical energy

necessary to convert a given amount of oleic acid into product can easily be calculated

from this equation in joules and converted to kW-hrs, the standard unit for calculating

electricity costs. An average commercial electricity cost for 2011 of \$0.1032/kW-hr was

used in this calculation [13].

3.2.4 Measurement of Fuel Properties

Approximately 150 mL of Hofer-Moest product converted from a technical oleic acid feedstock, containing 80% oleic acid and 20% other LCFA's, was produced and extracted. This sample was sent to Dr. Robert O. Dunnwith the United States Department of Agriculture's (USDA) National Center for Agricultural Utilization Research (NCAUR) in Peoria, Illinois. ASTM standard tests referenced in ASTM D6751-11b were performed on this product and compared to results of testing on biodiesel derived from soybeans.

An additional 10 mL of the product was saved for higher heating value (HHV) testing. A Parr® 1241 Oxygen Bomb Calorimeter was used in an atmosphere of O_2 at 30 psi to measure the HHV of the fuel. This test was done in triplicate to produce reproducibility, using approximately 2.0 g of fuel for each test.

3.3 Results and Discussion

3.3.1 Reactor Setup and Polarity Switching

During every electrolysis, an initial drop-off in current was noted in the first 30 seconds. This was hypothesized to be caused by the rapid saturation of the anodic surface by reaction product, making the diffusion of anions to the electrode surface the rate-limiting step of the reactions, causing resistance in the current. Switching polarities periodically was found to significantly improve currentdrop-off because hydrogen gas formation on the cathode surface (previously the anode) helped to remove product off of the electrode surface. In the cookie jar reactor, switching polarities every 10 seconds was found to increase the total charge in an identical electrolyte by 36%.

Identical oleic acid electrolytes were tested in the pump reactor, and current densities (current/surface area) were compared. A current density of 0.010 A/cm^2 was noted for the vertical electrode pack with 3 mm spacing after three minutes of electrolysis, compared to only 0.003 A/cm^2 for the horizontal electrode pack in the bucket with 0.8 mm spacing. It is suspected that the wider spacing and vertical orientation allowed the product to be more easily removed than the horizontal pack, which seemed to trap the product on the surfaces, with the sheer force not working as planned. By using the density and viscosity of methanol and the hydraulic diameter of the openings of the horizontal electrode pack on the inner and outer diameters, Reynolds Numbers of less than 2100 were calculated, signifying laminar flow throughout the pack.

In a parallel circuit, each electron counted in the current will have only passed through one electrochemical cell. In series, it will have passed through five electrochemical cells. However, in this system, only 1/5 of the voltage necessary in the series configuration is necessary to produce the same cell potential in a parallel configuration. To maximize the volume of the reactor compared to the size of the electrode pack, experiments were done with identical electrolytes to test series vs. parallel. The graph in Figure 3.5 shows the current recorded during 10 minutes of electrolyses of identical oleic acid electrolytes in the cookie jar reactor, comparing series and parallel configurations with no polarity switching.
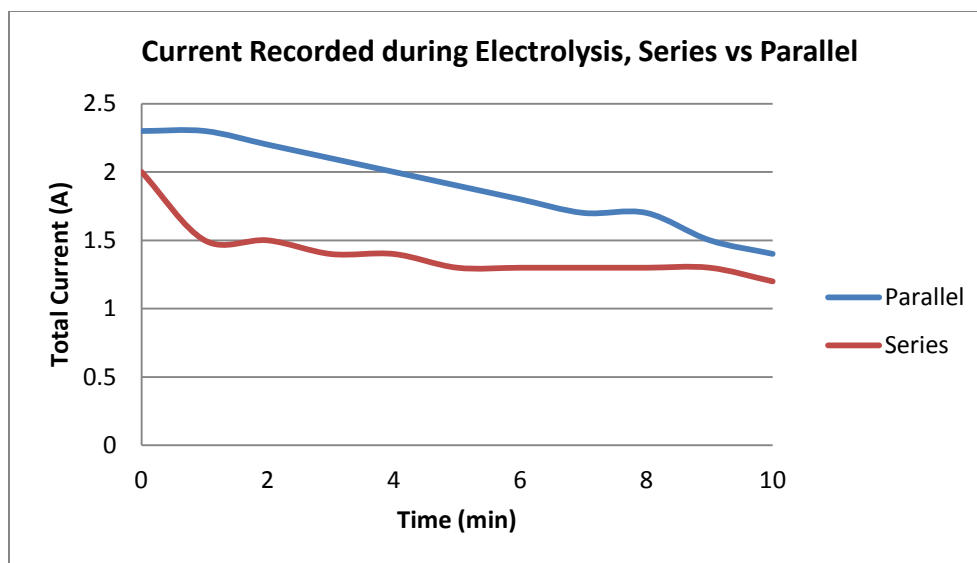
Figure 3.5: Comparison of series vs. parallel currents using the cookie jar reactor and

identical electrolyte solutions

Although a higher current is recorded in parallel, it is not close to five times the

current recorded in the series configuration, as would be expected. A reactor in series is

much more efficient when considering a space-time yield, as it is producing

approximately five times the amount of product per ampere. This drop in efficiency in

the parallel circuit can be explained by the effects of resistive heating, also known as

ohmic or Joule heating. Some of the electrical energy input will be converted to heat

rather than current. This heat, Q, is proportional to the current (I) squared times the

resistance (R) [4]. Note that the Q in Equation 3.5 is a variable for heat, not total charge.

$$Q_{resistive} \propto I^2 \cdot R \qquad\qquad \textbf{[3.5]}$$

Due to the increased current in a parallel configuration, much more of the electrical

energy is sacrificed to heating losses. Tighter spacing in a parallel circuit would likely

improve the total current, and, therefore, the rate of production.

3.3.2 Minimum Reaction Potential

The GC/MS results for these experiments are shown in Figures 3.6-3.8 for 2.0 V/cell, 2.5 V/cell, and 3.0 V/cell, respectively. A very clear result is shown in that no peaks are evident at 2.0 V/cell, but the expected pattern of peaks is clear at 2.5 V/cell and even more emphasized at 3.0 V/cell. This signifies that the electrochemical reactions of this system begin at cell voltages between 2.0 V and 2.5 V, and obviously proceed at a greater rate at higher voltages (or potentials). It is important to note that this is not the standard reduction potential of the reaction vs. Standard Hydrogen Electrode (SHE). Overpotential effects are present in this experiment, which make this result only applicable to this particular electrode setup and set of reaction conditions. The overvoltage caused by hydrogen gas formation at the cathode alone is at least 0.6 V/cell [2]. For comparison, critical cell potentials for the decarboxylation of various short chain fatty acids vs. SHE have been observed between 2.1 and 3.0 V in aqueous solutions on platinum electrodes [14].
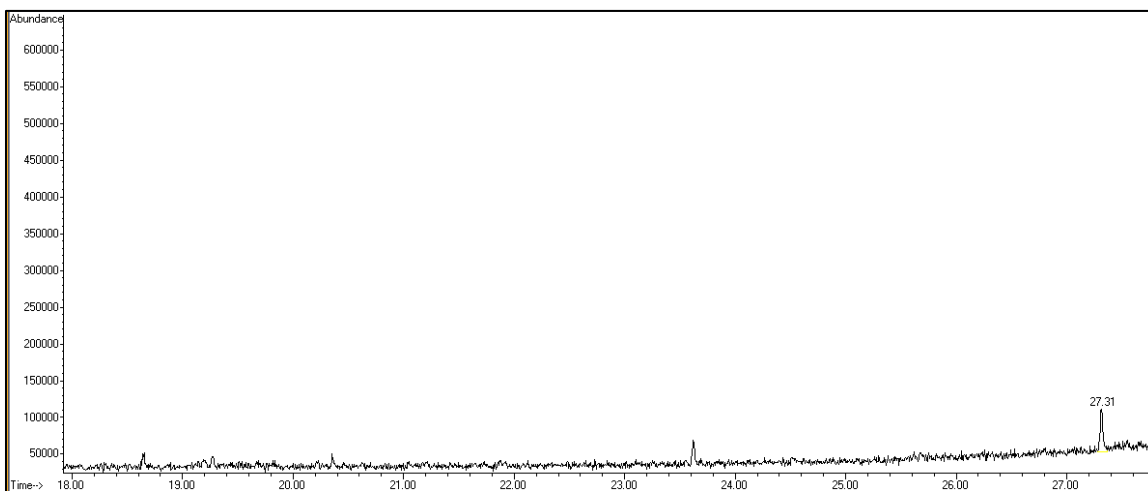

Figure 3.6: Lack of any product peaks after 30 min. electrolysis at 2.0 V/cell
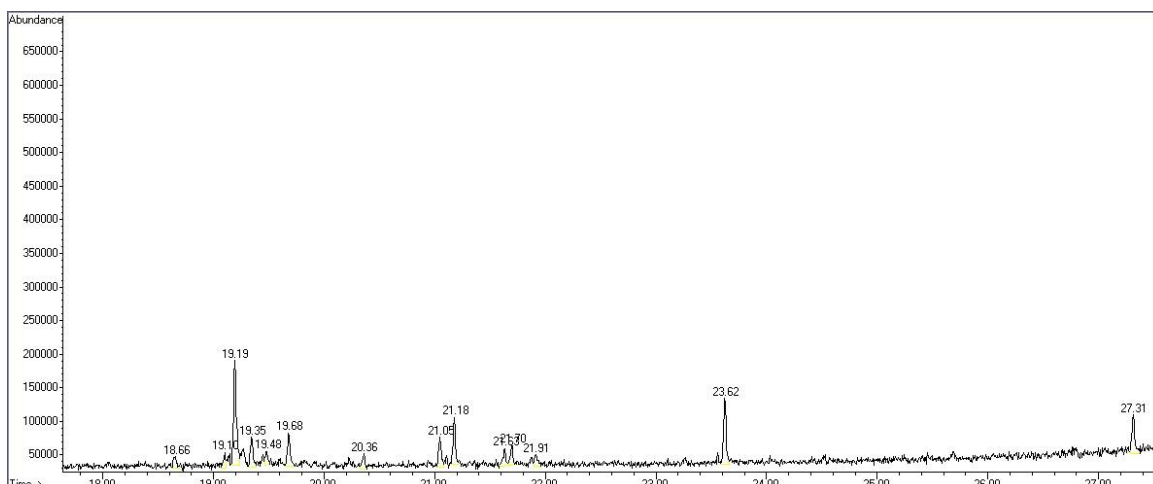
Figure 3.7: Small concentration of product after 30 min. electrolysis at 2.5 V/cell
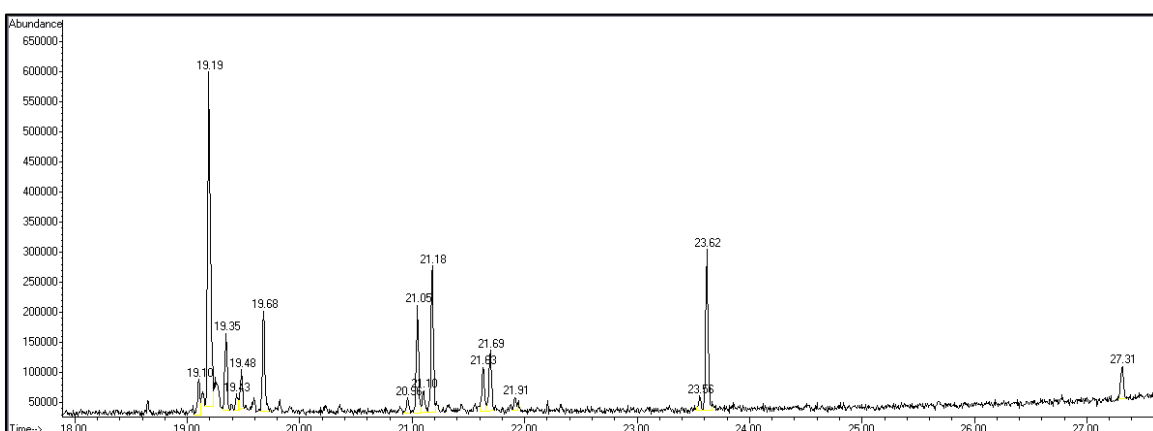

Figure 3.8: Increase in product concentration after 30 min. electrolysis at 3.0 V/cell

3.3.3 Current Efficiency and Costs

After 120 minutes of electrolysis in the cookie jar operatedin a parallel configuration, 5.18 g of product was separated. This represented approximately 5.02 g of electrochemical product and 0.16 g methyl esters, as found through GC/MS analysis. Assuming a distribution similar to that in Table 2.2, an average molecular weight of 244.5 g/mol was calculated for the electrochemical product. Using Newton-Cotes closed integration methods, a total charge of 5362.7 C was calculated by numerically integrating

the current over time. From Chapter 2, the Hofer-Moest reaction involves a two-electron

transfer. Using this information, the following calculation from Eq. 3.2 gives a total

theoretical mass that could have been produced, assuming 100% current efficiency.

$$m_{theoretical} = \frac{Q \cdot MW}{n \cdot F} = \frac{5362.7\ C \cdot 244.5\ g/mol}{2 \cdot 96485\ C/mol} = 6.79\ g$$

From the calculated $m_{theoretical}$ and the measured m_{actual}, a current efficiency (CE) of

73.9% was found for the process. The other current in the system can likely be attributed

to the electrolysis of water or methanol, which tends to increase as more hydroxide and

methoxide ions are present in solution, as discussed in Chapter 2.

Electrical energy costs were then estimated using Eq. 3.4. During the 120

minutes of the current efficiency experiment, 21450.8 J (or 5.96 x 10^{-3} kW-hrs) of

electrical energy were consumed. Using the average 2011 commercial rate of

$0.1032/kW-hr, $0.000615 of electricity was consumed to produce 5.18 g of product, for

an average of $0.000119/g or $0.119/kg. Using an average density of 0.85 g/mL for the

product [15], an electrical energy cost of $0.101/L or $0.383/gallon is calculated. It is

important to note that other pre-processing and refining costs will be included in the

process, so this is not the only associated cost with the potential fuel production.

3.3.4 Measurement of Fuel Properties

Dr. Dunn's results for the fuel tests and the HHV results of the Hofer-Moest

product from technical oleic acid are compared to soybean biodiesel and No. 2 petroleum

diesel, included below in Table 3.2 [16]. It is important to note that these tests performed

were developed for biodiesel, not Hofer-Moest products.

	Hofer-Moest Product	Soybean Biodiesel	No. 2 Petroleum Diesel
Higher Heating Value (HHV), kJ/kg	42,212 ± 2,027	39,628	43,382
Cloud Point (°C)	-7.4	0.1	-15 to 5
Pour Point (°C)	-27	-1	-35 to -15
Induction Period (hours)	0.50	2.59	>24
Water content (ppm)	626	456	-
Acid value (mg KOH/g oil)	67	0.26	-

Table 3.4: Fuel properties of Hofer-Moest products compared to biodiesel and

petrodiesel

The Hofer-Moest products have better heating value and cold flow properties than

biodiesel, more similar to petrodiesel. The fuel does have problems with oxidative

stability (as measured by induction period), water content, and acid value, though. The

water content and acid value can easily be fixed by improving refining methods in

commercial use. The induction period is not as simple. The instability of the molecules

is attributed to the many olefins (in this case of technical oleic acid product, non-

conjugated dienes or diolefins) found in the product mix. The double bonds increase

molecular instability, especially at the temperature (110°C) where the induction period

testing takes place. The trend of decreasing induction period with increasing unsaturated bonds is seen in biodiesel data as well, presented by Knothe [8] and shown here in Table 3.5.Fuel additives which improve oxidative stability are available, which would help this property, as would a higher degree of saturation [17].

Biodiesel product	Induction period (hrs)
Methyl stearate (18:0)	>24
Methyl oleate (18:1)	2.79
Methyl linoleate (18:2)	0.94
Methyl linolenate (18:3)	0

Table 3.5: Trend of increasing induction period with increasing degree of saturation in biodiesel molecules, as presented by Knothe [8]

3.4 Conclusions

Non-Kolbe electrolysis and the Hofer-Moest reaction is an intriguing idea for renewable fuel production. A hydrocarbon fuel is produced, with some important properties superior to those of biodiesel, e.g. heating value and cold flow, while others, namely oxidative stability and fuel refinement, are made even worse. The results of electrochemical current efficiency and economics of the electrical energy consumption of the process seem reasonable, so long as the other costs associated with production such as production of feedstocks, pre-processing, and refinement do not make the process uncompetitive.

3.5 References

[1] Prentice, G. (1991). Electrochemical Engineering Principles, xi-xiv, Prentice Hall.

[2] Mantell, C. L. (1968). Electro-Organic Chemical Processing, Noyes Development Corporation.

[3] Goodridge, F.; Scott, K. (1995). Electrochemical Process Engineering, 194-197, Plenum Press.

[4] Lund, H.; Baizer, M. M. (1990). Organic Electrochemistry: An introduction and guide, 3rd edition, Marcel Dekker, Inc.

[5] Rifi, M. R.; Covitz, F. H. (1974). Introduction to Organic Electrochemistry, Marcel Dekker, Inc.

[6] Boshui, C.; Yuqiu, S.; Jianhua, F.; Jiu, W.; Jiang, W. (2010). Effect of cold flow improvers on flow properties of soybean biodiesel, Biomass and Bioenergy, 34, 1309-1313.

[7] Dunn, Robert O. (2011). Fuel properties of biodiesel/Ultra-Low Sulfur Diesel (ULSD) Blends, J Am Oil ChemSoc, 88, 1977-1987.

[8] Knothe, G. (2009).   Improving biodiesel fuel properties by modifying fatty ester compositions, Energy & Environmental Science, 2, 759-766.

[9] ASTM International. (2011). Standard specification for biodiesel fuel blend stock (B100) for middle distillate fuels, D6751-11b.

[10] ASTM International. (2010). Standard specification for diesel fuel oil, biodiesel blend (B6 to B20), D7467-10.

[11] ASTM International. (2012). Standard specification for diesel fuel oils, D975-11b.

[12] Chapra, S. C.; Canale, R. P. (2002). Numerical Methods for Engineers, 4th Edition, 596-604, McGraw-Hill Companies, Inc.

[13] U.S. Energy Information Administration. (2011). Table 5.3: Average Retail Price of Electricity to Ultimate Customers: Total by End-Use Sector, U.S. Department of Energy.

[14] Eberson, L.(1969). Electrochemical reactions of carboxylic acids and related processes, *The Chemistry of Carboxylic Acids and Esters (Patai, S.),* 53-103.

[15] Alptekin, E.; Canakci, M. (2008). Determination of the density and the viscosities of biodiesel-diesel fuel blends, Renewable Energy, 33, 2623-2630.

[16] Joshi, R. M.; Pegg, M. J. (2007). Flow properties of biodiesel fuel blends at low temperatures, Fuel, 86, 143-151.

[17] Kenreck, G. (2007). Improving biodiesel stability with fuel additives, Biodiesel Magazine, http://www.biodieselmagazine.com/articles/1443/improving-biodiesel-stability-with-fuel-additives/

Chapter 4 – Feedstocks and Conclusions

Using non-Kolbe electrolysis for production of renewable diesel offers a huge advantage over other methods due to the robustness of feedstocks that can be used to produce fuel. Whereas production of biodiesel requires a feedstock with low FFA and water, this electrolysis could thrive with waste feedstocks such as yellow and brown greases, animal fats, algae oils, sludge-extracted lipids, or biodiesel salt wastes, which contain increased amounts FFA's and moisture compared to virgin oils.

This project offers much promise in creating a high quality renewable diesel fuel from fatty acids. Competitive economics and promising fuel quality are advantages. However, much work remains, especially in the areas of separations and optimization of process conditions, to determine if this is a viable waste-to-diesel fuel conversion process.

4.1 Introduction

An important advantage of using non-Kolbe electrolysis for the conversion of fatty acids to renewable diesel is the robustness of feedstocks which can be fed to the process. Whereas biodiesel requires an anhydrous and low FFA source of triglycerides (in most literature results, <4% FFA content) for transesterification [1], no problems have been noted with the electrolysis in electrolytes with a high water content (up to 25%), and FFA's are actually desired for conversion to salts and subsequent decarboxylation. Acid-catalyzed esterification offers an alternative to transesterification to yield alkyl esters from both triglycerides and FFA's, but problems with slow reaction times and high water content feedstocks limit the commercial applications of the method [2]. In biodiesel production, high FFA feedstocks can be processed through a two-step process: first, FFA are converted by acid-catalyzed esterification, which selectively esterifies FFA's before triglycerides. Subsequently, triglycerides are converted to biodiesel with a basic catalyst. However, this additional pretreatment step adds additional process steps, energy inputs, and costs, and still cannot be used on feedstocks with FFA content greater than 10% due to formation of water [1].

Solid acid catalysis is another process which has shown progress in treating high FFA feedstocks. It offers advantages in both that the heterogeneous catalyst offers easier separation and that it does not lead to the corrosion of process equipment, as a homogeneous acid catalyst does. Mixtures of triglycerides and FFA's could be converted to alkyl esters, as with homogeneous acid catalysts. However, there are still problems with finding a suitable catalyst which is stable under reaction conditions and dealing with

wastes with high water content without inputting a large amount of energy to dry

feedstocks [3,4]. This is currently an active area of research.

4.2 Potential Feedstocks

Two problems that have plagued the biodiesel industry are the costs of feedstocks

and concerns about negative net energy balances (NEB). When producing biodiesel from

virgin feedstocks with a low FFA content, both the costs and energy inputs of farming

crops, which are substantial, must be taken into account. These virgin feedstocks often

are used for food as well, so competitive use drives up cost even further, both for the food

and fuel feedstock. By utilizing wastes or other feedstocks that are not farmed and have

limited additional uses, the cost of the feedstock is driven down and avoiding the deposit

of this waste in a landfill is actually a positive input on the energy balance for the

process. The Global Warming Potential (GWP) of such waste utilization processes is far

less than production of biodiesel from virgin feedstocks [5]. The following feedstocks,

which have potential problems in biodiesel transesterification, could fit into the

electrochemical conversion process well.

4.2.1 Yellow and Brown Greases and Animal Fats

Recent statistics indicate that 11.638 billion pounds of waste fats are produced

each year in the US, which has the potential to be converted to 1.5 billion gallons of

renewable diesel fuel [6]. Much of this is either from waste cooking oils or meat-

processing facilities. These wastes have high FFA and moisture contents. Waste oils that

contain less than 15% FFA are considered "yellow grease". Those with over 15% FFA

are considered "brown grease". A sample of animal fat was reported to have 25.7% FFA's, a similar composition to many brown greases [7]. Moisture content in the grease wastes was found to vary between 0.01% and 55.38%. A two-step process involving acid esterification followed by base transesterification has been reported to successfully reduce the FFA content to less than 1% in both yellow and brown greases with low moisture contents, but requires time-consuming separation steps and corrosive reaction conditions [7].

Two possible methods of using non-Kolbe electrochemical conversion could produce useful fuels from both FFA's and triglycerides simultaneously. The first is to convert all fats into FFA salts through hydrolysis with an aqueous base, a process known as saponification, as shown in the reactions in Figures 1.12 and 1.13, producing glycerol from the triglyceride hydrolysis. All of these salts could then be converted into Hofer-Moest products in an electrolyte consisting of some combination of methanol, water, and glycerol. The other method would be to subject the waste to the combination of methanol and sodium hydroxide. This would produce some methyl esters (biodiesel) and glycerol from most of the triglycerides, and salts from the other triglycerides and FFA. By using an excess of methanol, the salts could be ionized in a combination of methanol, glycerol, and water and converted to Hofer-Moest products through electrolysis. The final fuel product of this process would be a blend of biodiesel and Hofer-Moest products.

4.2.2 Algae Oil

As outlined in Section 1.2.3, algal oils have the potential to become an important source of biofuel feedstocks, mainly due to their yield of oils per acreage of land used.

Many strains of algae exist, each of which synthesizes a unique combination of lipids [8]. Although much effort has been devoted to characterizing algae fatty acids by chain length and saturation, no literature was found comparing triglyceride content to FFA's in algae. A sample of algae oil procured during this research yielded approximately 35% FFA's by separating the FFA's and triglycerides based on polarity. With the aquatic nature of algae, much energy must be dedicated to drying oils for biodiesel production. The ability to convert feedstocks with high FFA oil and water content is an advantage which non-Kolbe electrolysis has in comparison to biodiesel production with algae oils.

4.2.3 Sludge Extractions

Extracting lipids from sludges for use as a renewable fuel is an exciting possibility, with the additional advantage of lessening the burden of disposal in landfills. *In situ* esterification experiments of municipal primary sludge with methanol and a sulfuric acid catalyst have reportedly yielded up to 14.5% fatty acid methyl esters (FAME or biodiesel), based on the dry weight of the sludge [9]. Given that approximately 6.2 x 10^6 tons of dried sewage sludge is produced per year in the US alone, a significant amount of fuel could be made from this process. A high content of phospholipids and FFA's are likely to be present in oils from sludge, due to the increased amount of oils extracted by a polar solvent (methanol) compared to a non-polar solvent (hexane) [10]. Given the apparent high FFA content and high moisture content present in most sludge, the electrochemical conversion process again makes sense as a conversion technology which would work with this feedstock.

4.2.4 Biodiesel Waste

During the transesterification of a lipid-based feedstock with a basic catalyst, any FFA's in the feedstock will form fatty acid salts. During the separation of biodiesel and the glycerol-based waste layer, most FFA salts settle into the waste with some of the excess alcohol left unused during the reaction. A typical waste composition after the production of biodiesel at the Bently Biofuels facility in Minden, Nevada is approximately 2/3rd glycerol and 1/3rd methanol with a concentration of fatty acid salts of about 5% [11]. These waste FFA salts can be converted into additional fuel through electrolysis. Figure 4.1 below shows the possible synergy between biodiesel production and the electrochemical process.
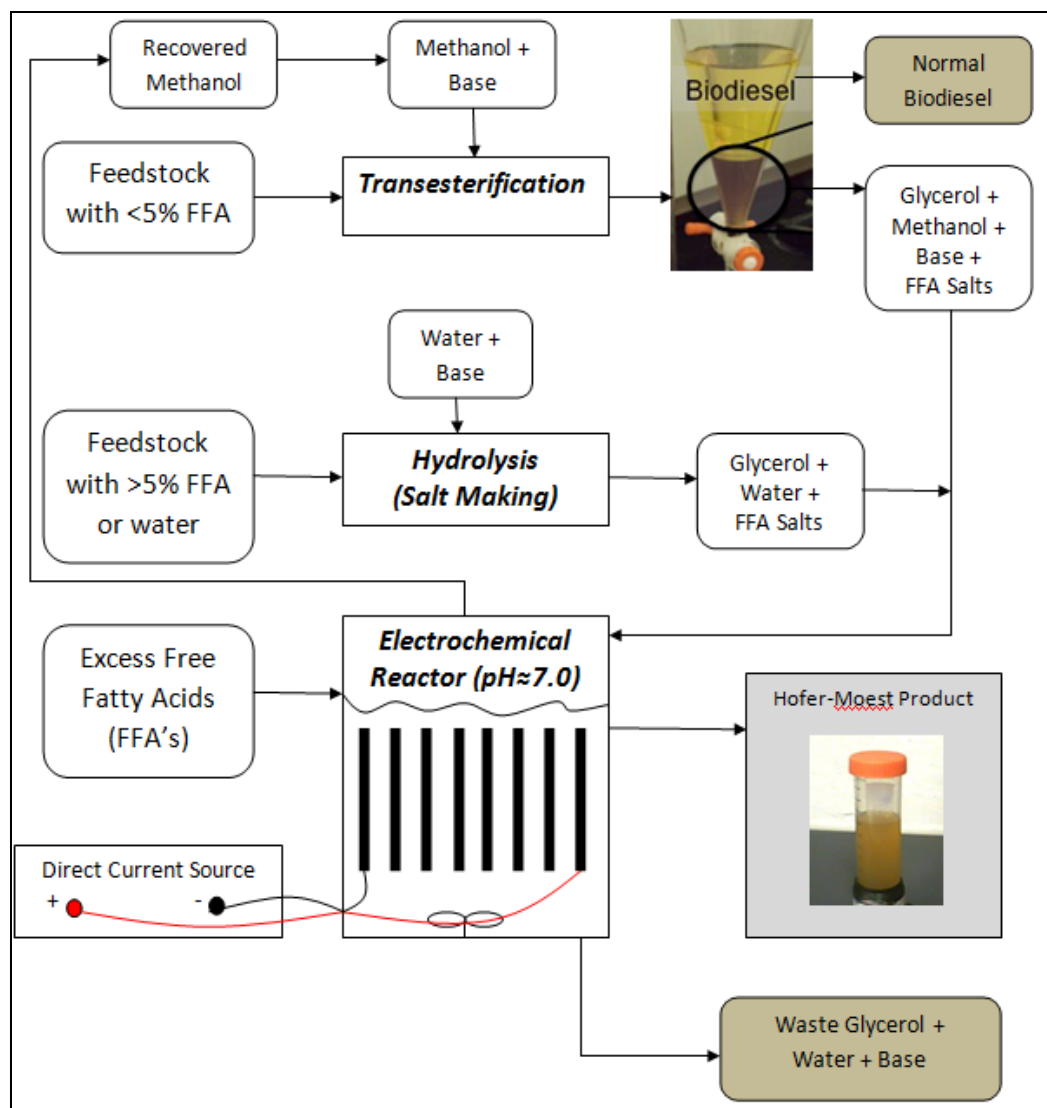
Figure 4.1: One embodiment of how non-Kolbe electrolysis could work with biodiesel production to produce additional fuel

4.3 Project Conclusions

Using non-Kolbe electrolysis and the Hofer-Moest reaction to convert FFA's to a renewable diesel fuel is an intriguing process. Conclusions from the overall scope of the

research work presented on this project lead to many possibilities for future developments of this technology.

A combination of hydrocarbons and ethers were found to be the main products from non-Kolbe electrolysis of long-chain fatty acids. This reaction was typically done in methanol, although electrolysis in ethanol and glycerol were also tested. Graphite electrodes in a reactor with undivided electrochemical cells promoted two-electron Hofer-Moest type reactions, which provided evidence of the existence of a brief carbenium ion during the reaction. Through varying temperature and pH, some selectivity towards certain products was determined. Higher temperatures demonstrated higher observed currents but decreased current efficiency.

Several modifications were made in the electrochemical reactor to optimize current densities. A vertical configuration of electrodes with 3 mm spacing resulted in increased current density, compared to horizontally configured electrodes with smaller spacing. An efficient way of maintaining current high current densities was to periodically switch polarities, causing electrode surfaces to change between acting as an anode and cathode.

An electrolysis of oleic acid salts demonstrated a 73.9% current efficiency, from which a price for electricity of $0.383 per gallon could be calculated. A 2.5 V/cell potential was necessary to drive the decarboxylation. This showed that the production of this fuel with electricity was feasible economically, although other price inputs (such as cost of feedstocks) should be considered.

Fuel testing of the product showed promising heating values and cold-flow properties but poor oxidative stability and purity. While the purity problems can be fixed

by better fuel refinement methods and a careful electrode setup where metals from copper wires do not contact the electrolyte, the oxidative stability is an uncontrollable effect related to the unsaturation of the product. Working with more highly saturated fatty acids or fuel additives should improve this oxidative stability. Overall, this method for producing fuel electrochemically showed promise, especially for feedstocks with high FFA or water content.

4.3.1 Recommendations for Future Research

Many challenges still exist in this process. The most obvious is in the separation of the products from the electrolyte. As with biodiesel processing, FFA salts cause problems in separations in this system, as well. A more efficient method of cleaving products off the surface of electrodes is also needed. Opening electrode surface space would increase current density, thus increasing production rate.

Electrochemical conversion of various waste streams has great potential. The ability of the system to handle a robust range of feedstocks with both high FFA and water contents is a huge advantage. All sorts of lipid-based wastes should be tested, especially cheap feedstocks such as brown greases and lipids extracted from sludge, to determine if a more economically feasible fuel production method than traditional biodiesel transesterification is possible. The effect of water concentration in the electrolyte should be examined more carefully, especially on current density and product composition.

A great deal of fuel testing is still needed. A more highly saturated product would be interesting to test, to find how much the oxidative stability improves. Blending the Hofer-Moest products with biodiesel to create a renewable blend would theoretically

improve the qualities in which both biodiesel and the Hofer-Moest products struggle independently. A 50/50 blend of biodiesel and Hofer-Moest products would be interesting to compare to petrodiesel.

Finally, more work must be done to understand the net energy balance (NEB) around the process. The NEB will be unfavorably affected by the additional electrical energy required through electrolysis, but some energy is likely to be saved through the decreased consumption of chemicals in comparison to production of biodiesel. Calculations of energy inputs inherent with various feedstocks would hopefully ensure that this process would not have similar struggles to US corn ethanol production. Even with waste feedstocks, the energy necessary to do any separation or pre-processing should be considered. The global need for some type of transportation fuel will increase in the near future, so developing this technology to offer an advantageous conversion process compared to biodiesel processing is worthwhile and could eventually be very lucrative.

4.4 References

[1] Vasudevan, P. T.; Briggs, M. (2008). Biodiesel production – current state of the art and challenges, J. Ind. Microbiol. Biotechnol., 35, 421-430.

[2] Suwannakarn, K.; Lotero, E.; Ngausuwan, K.; Goodwin, J. G. (2009). Simultaneous free fatty acid esterification and triglyceride tranesterification using a solid acid catalyst with *in situ* removal of water and untreated methanol, Ind. Eng. Chem. Res., 48, 2810-2818.

[3] Kiss, A. A.; Dimian, A. C.; Rothenberg, G. (2006). Solid acid catalysts for biodiesel production – Towards sustainable energy, Adv. Synth. Catal., 348, 75-81.

[4] Lotero, E.; Liu, Y.; Lopez, D. E.; Suwannadarn, K.; Bruce, D. A.; Goodwin, J. G. (2005). Synthesis of biodiesel via acid catalysis, Ind. Eng. Chem. Res., 44, 5353-5363.

[5] Dufour, J.; Iribarren, D. (2012). Life cycle assessment of biodiesel production from free fatty acid-rich wastes, Renewable Energy, 155-162.

[6] Canakci, M. (2005). The potential of restaurant waste lipids as biodiesel feedstocks, Bioresource Technology, 1-8.

[7] Canakci, M.; Van Gerpen, J. (2001). Biodiesel production from oils and fats with high free fatty acids, Transactions of the ASAE, 44, 1429-1436.

[8] Krohn, B. J.; McNeff, C. V.; Yan, B.; Nowlan, D. (2011). Production of algae-based biodiesel using the continuous catalytic Mcgyan® process, Bioresource Technology, 102, 94-100.

[9] Mondala, A.; Liang, K.; Toghiani, H.; Hernandez, R.; French, T. (2009). Biodiesel production by *in situ* transesterification of municipal primary and secondary sludges, Bioresource Technology, 100, 1203-1210.

[10] Dufreche, S.; Hernandez, R.; French, T.; Sparks, D.; Zappi, M.; Alley, E. (2007).

Extraction of lipids from municipal wastewater plant microorganisms for production of

biodiesel, J. Amer. Oil Chem. Soc., 84, 181-187.

[11] Luri, Carlo. Personal interview. Feb. 12, 2012.

Appendix – Mass Spectroscopy Results from Hofer-Moest Product Peaks in Palmitic and Oleic Acid

A.1 MS Spectra for Palmitic Acid Products

The following are the fragmentation patterns for each peak identified in Table 2.2 for the palmitic acid product.
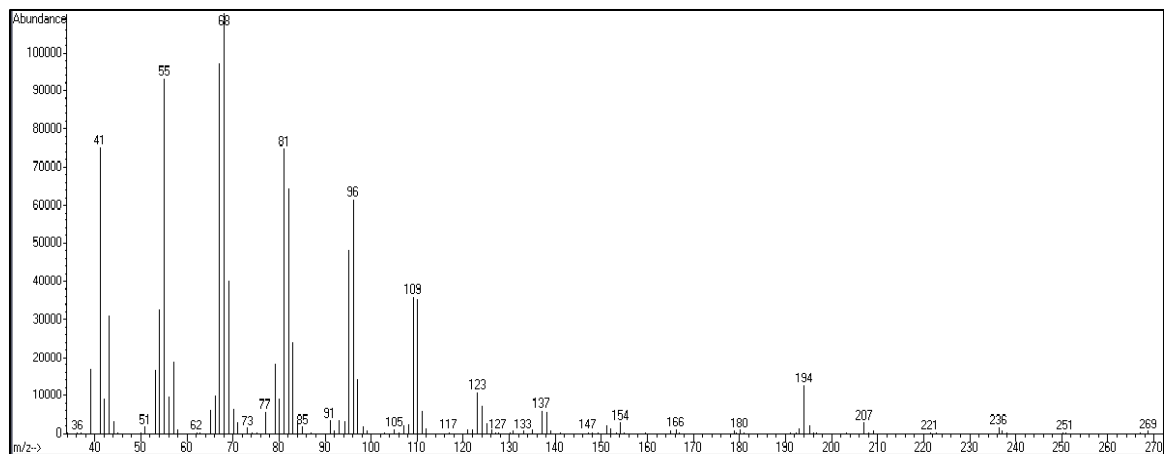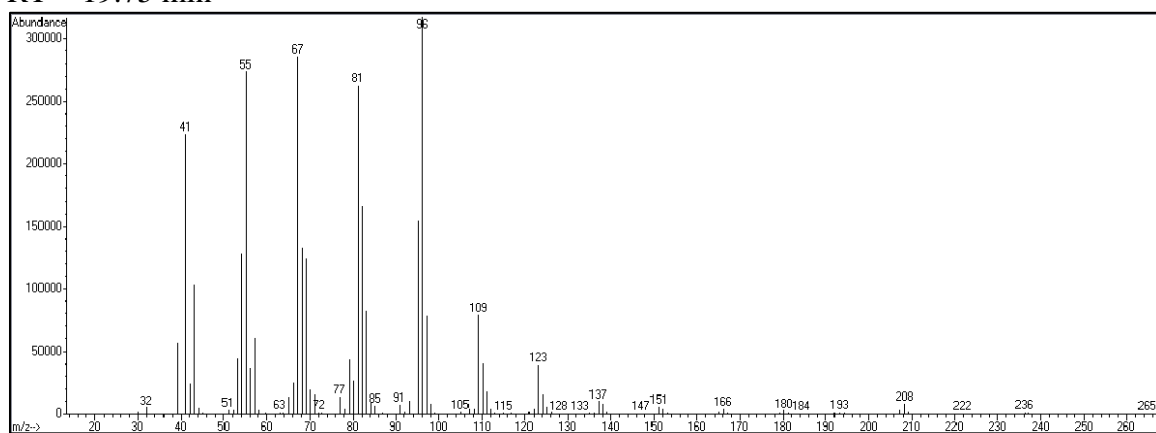
RT = 17.04 min
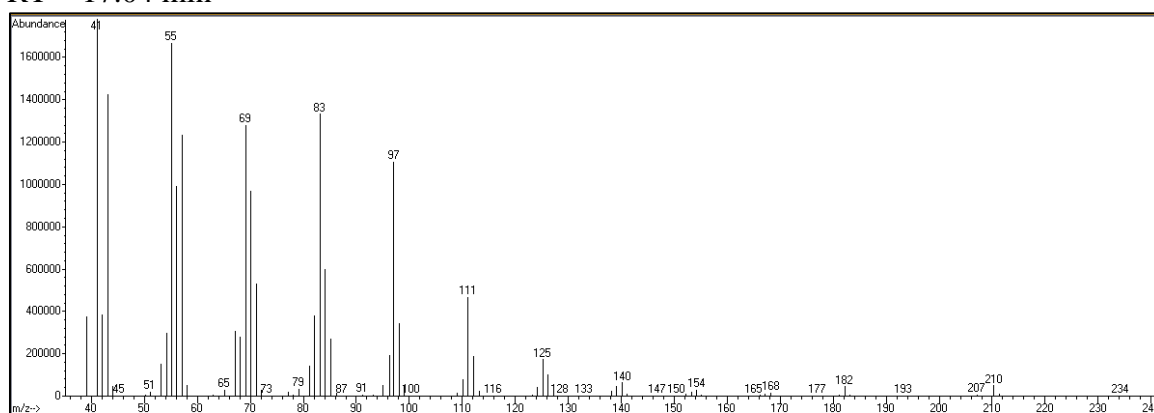
RT = 17.12 min
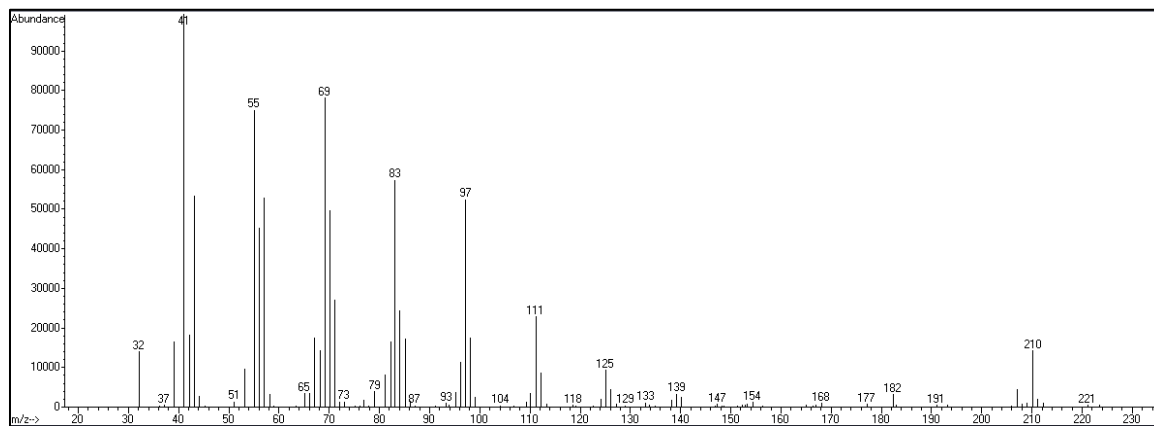
RT = 17.19 min
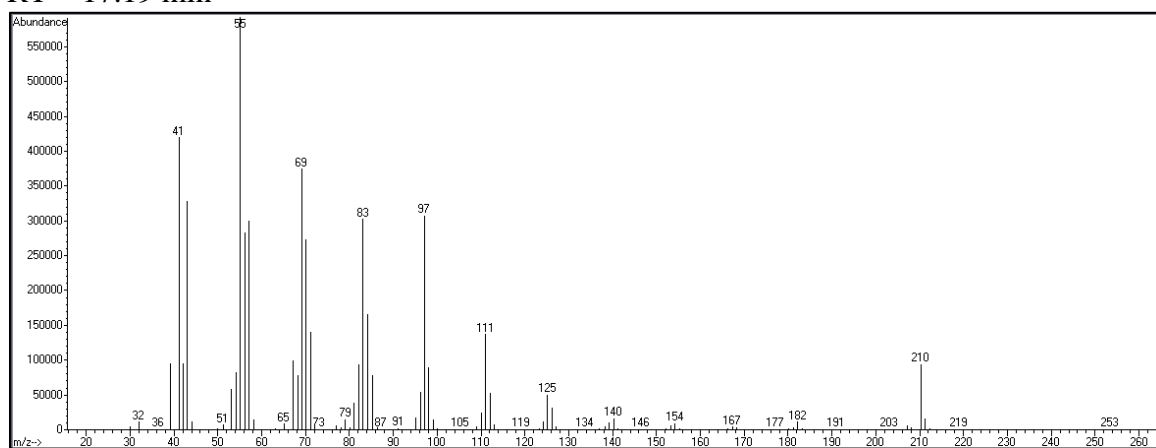
RT = 17.33 min
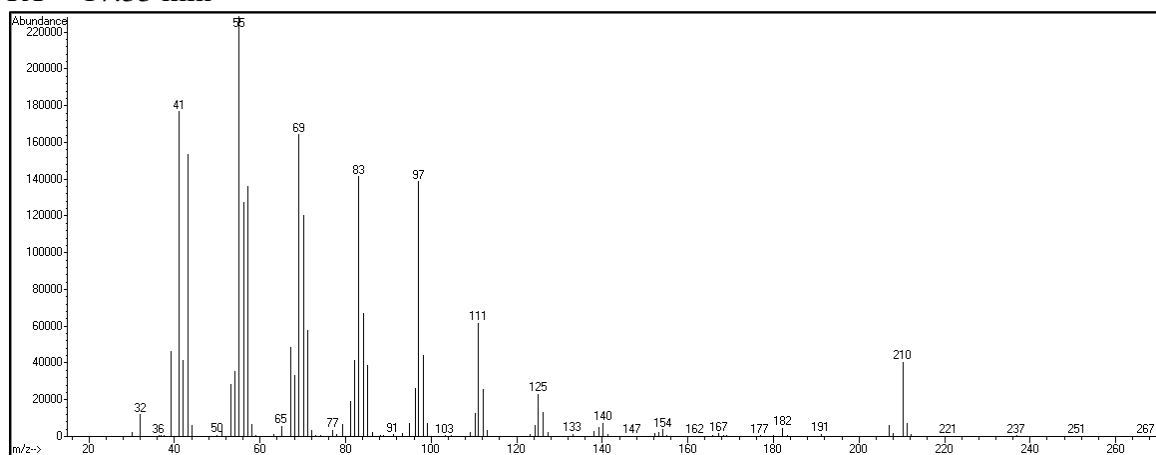
RT = 17.54 min
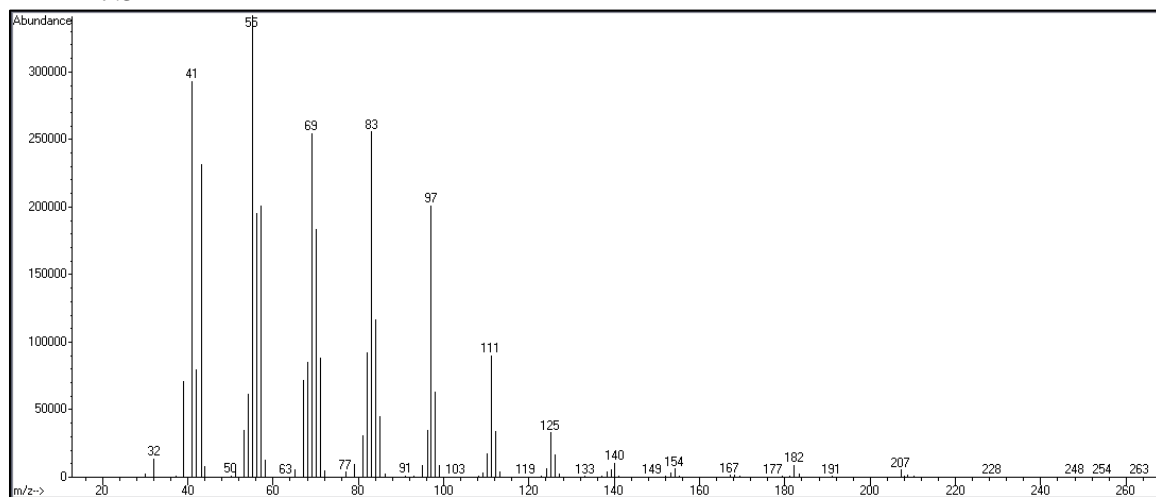
RT = 19.14 min
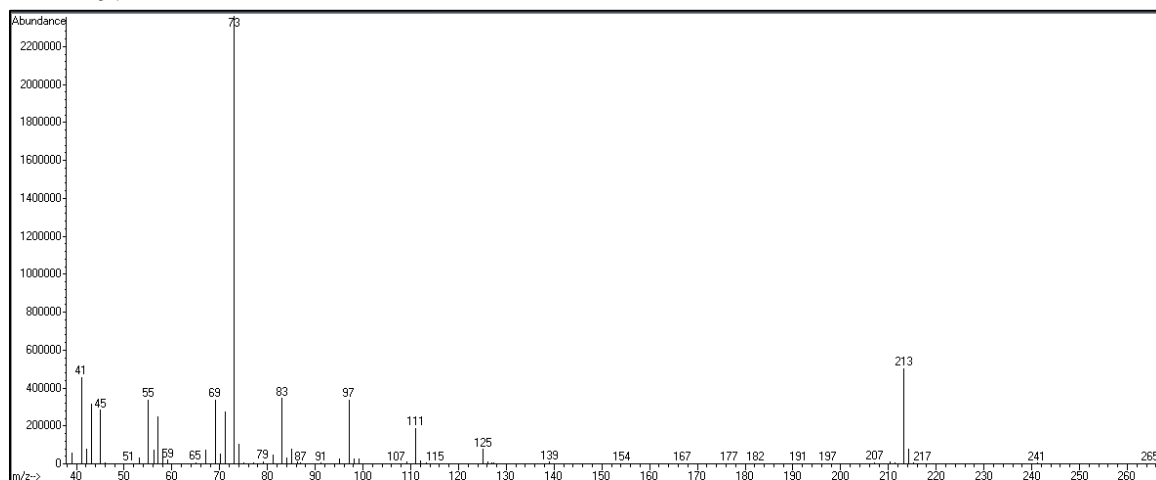
RT = 19.27 min
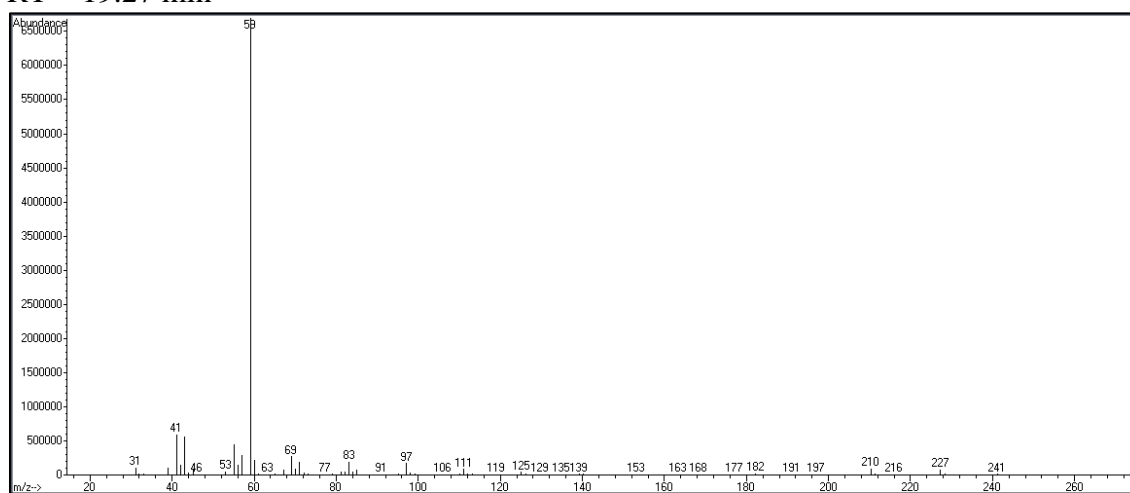
RT = 19.82 min
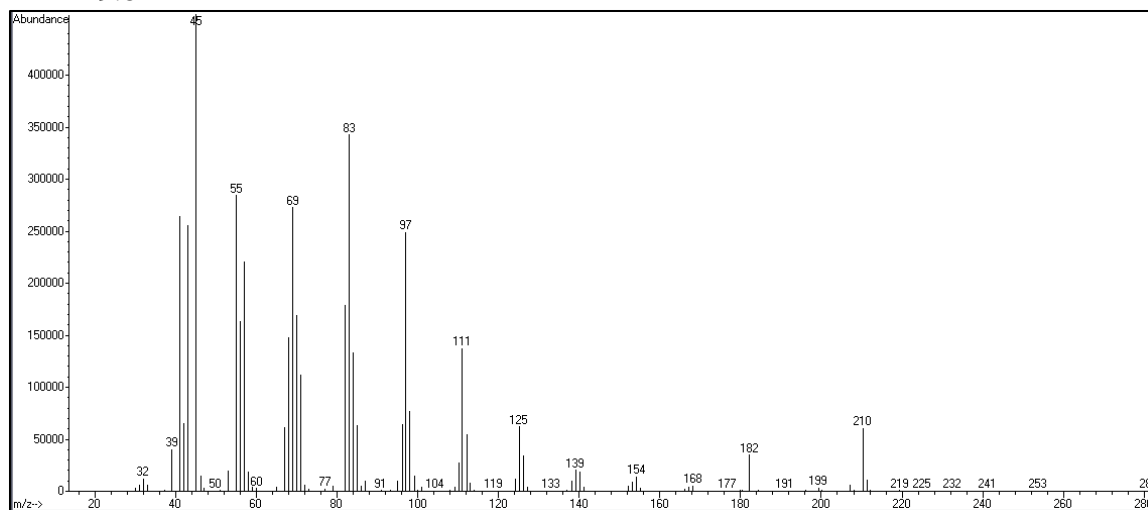
RT = 21.91 min
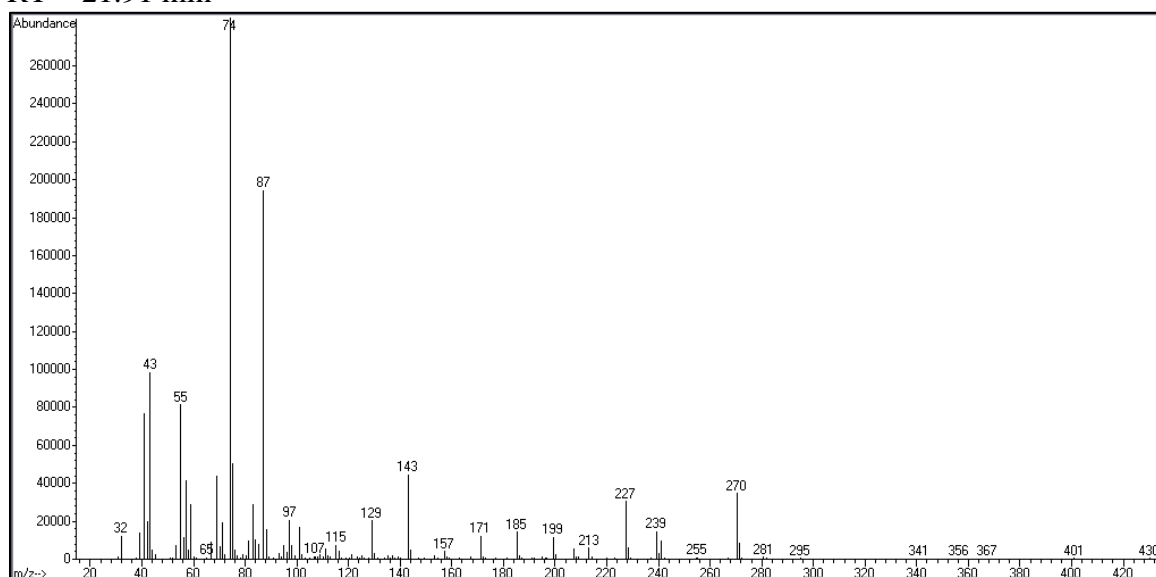
A.2 MS Spectra for Oleic Acid Products

The following are the fragmentation patterns for each peak identified in Table 2.2 for the oleic acid product.

RT = 19.26 min
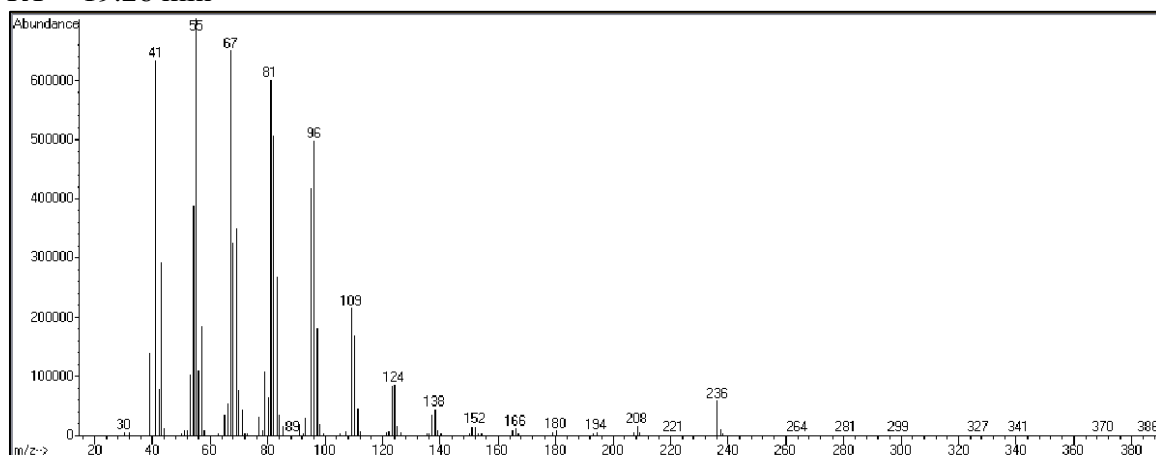
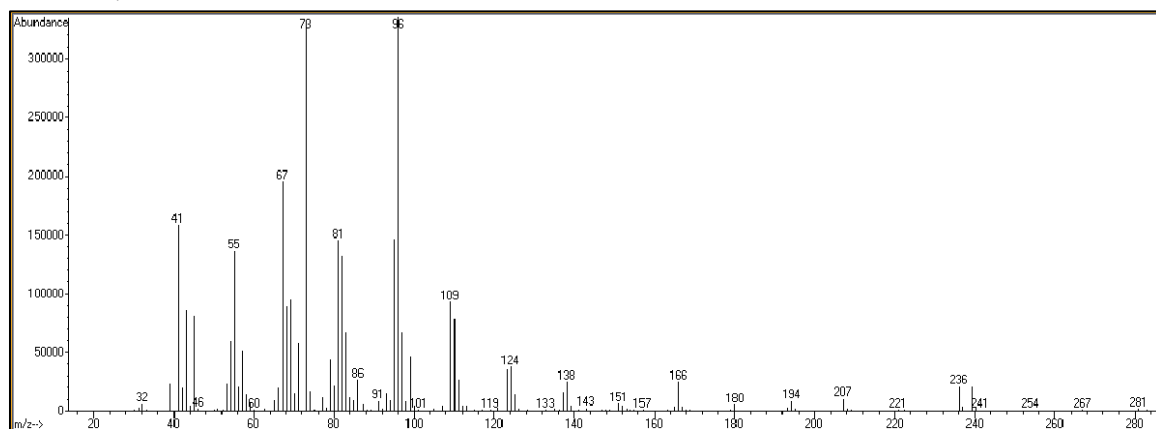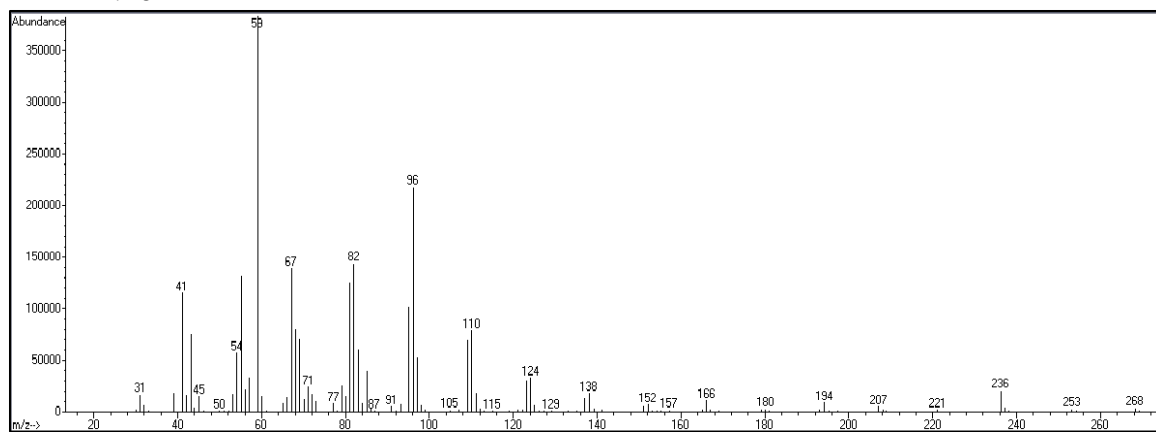RT = 19.33 min
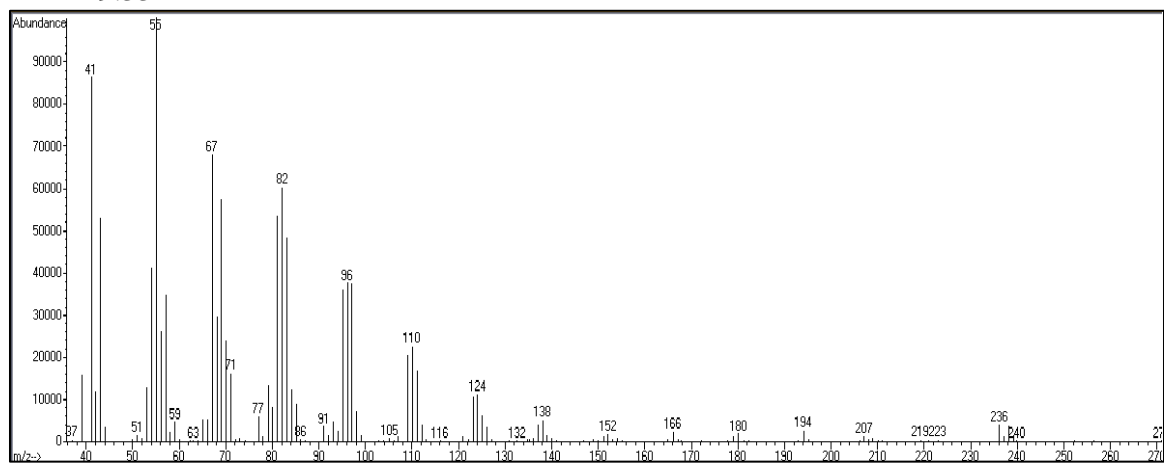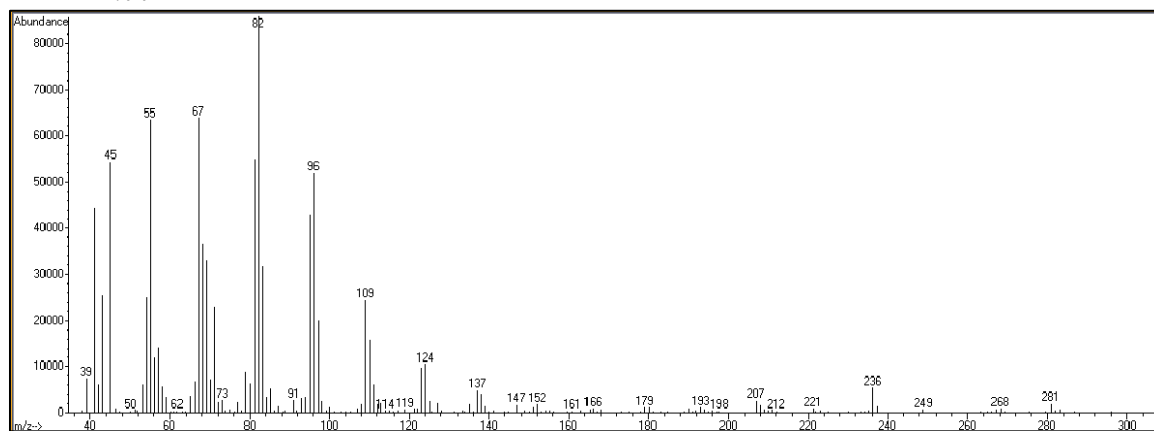

RT = 19.41 min
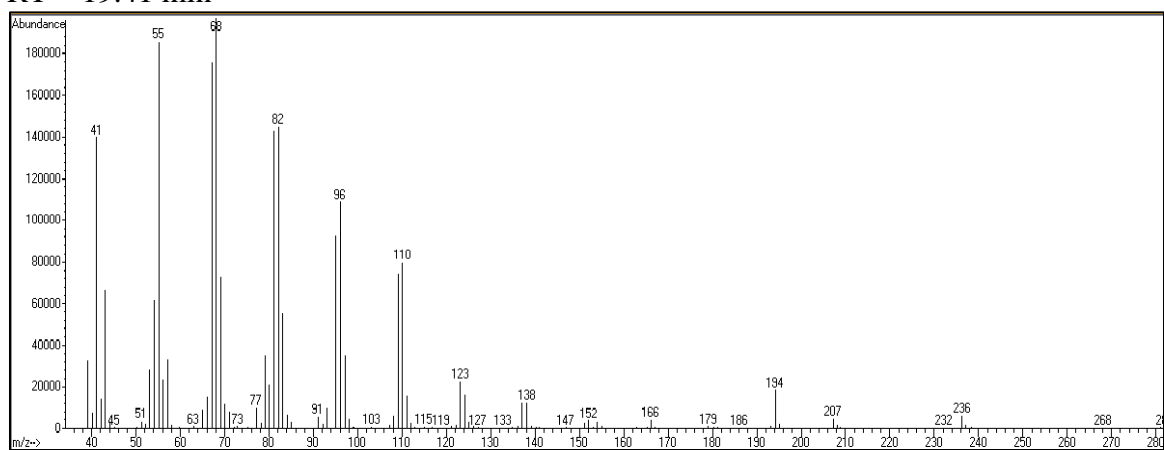
RT = 19.55 min

RT = 19.75 min

RT = 21.12 min

RT = 21.26 min

RT = 21.77 min

RT = 23.70 min